DNA VACCINES AGAINST HIV-1: AUGMENTING IMMUNOGENICITY OF gp120

A Thesis

Submitted to the Faculty of the

WORCESTER POLYTECHNIC INSTITUTE

In Partial Fulfillment of the Requirements for the

Degree of Master of Science

In

Biology

By

Diego José Farfán Arribas

DECEMBER, 2001

APPROVED:

Shan Lu, M.D, Ph.D. Major Advisor UMass Dept. of Medicine	David S. Adams, Ph.D. Committee Member	Joseph C. Bagshaw, Ph.D. Committee Member

ABSTRACT

There is currently no protective vaccine against HIV. It is known that a high mutation rate and the existence of many subspecies or clades generated by point mutations or recombination events, are at least partly responsible for the ability of the virus to escape immune responses elicited by classical vaccines. Protein subunit vaccines may not be effective due to this pronounced viral mutability. An immune evasion mechanism has been postulated in which variable domains occlude conserved epitopes crucial for infectivity. The use of DNA vaccines appeared as a favorable approach.

Here, a DNA vaccine approach is presented in which the DNA constructs have been engineered to circumvent the aforementioned problems by 1) introducing elements to enhance expression, such as a heterologous promoter, a heterologous signal sequence and intron sequences, 2) by optimizing codon usage, and 3) by vaccinating with antigens that have a modified glycosylation pattern which will make them more immunogenic. The results indicated that deglycosylation of different clades of gp120 did not affect the protein conformation, and '*in vitro*' expression levels were good. Antigen codon optimization dramatically increased antibody production. In the animals vaccinated with non-codon-optimized constructs, the presence of an intron and a heterologous signal sequence was required to achieve a good antibody response. Therefore, antigen engineering is required to obtain a powerful immune response against HIV-1 gp120.

TABLE OF CONTENTS

LIST OF FIGURES AND TABLES

ACKNOWLEDGEMENTS

I would like to thank, first and foremost, my mentor Dr. Shan Lu, who sets an extraordinary example of a life committed to biomedical research, and who gave me a vow of confidence and the opportunity to be involved in such a project. I feel very grateful to Dr. Shixia Wang as well, for her constant support for the duration of my thesis research. I would like to thank also all the other members of the Laboratory of Nucleic Acid Vaccines at the University of Massachusetts Medical School for their contribution to my technical training and for providing the wild-type gp120 clones and the clones used in the mouse experiment. Finally, I would like to express my gratitude to my committee members, Dr. Adams and Dr. Bagshaw. I feel grateful to Dr. Adams for his support and thesis revisions, and for putting me in contact with Dr. Lu, thus contributing to making possible my off-campus research experience.

BACKGROUND

DNA Vaccines

DNA vaccines consist of transient transfection of naked DNA into target cells. The main advantage lies on the fact that the proteins are expressed by the host's cells. Unlike subunit protein vaccines, DNA vaccines are an effective means to elicit cell immunity, since the antigens are produced inside the host's cells and are therefore presented via the MHC-I pathway. The secreted proteins can also reach professional antigen presenting cells (APCs) triggering MHC-II presentation.

It has been shown that exogenous proteins can also be presented via MHC-I in APCs to some extent (Watts, 1997), although these cells usually uptake antigen protein from the extracellular space, and present peptides via MHC-II. It is believed that both MHC-I and MHC-II presentation pathways are required for an effective immune response in which both specific antibody and cytotoxic T lymphocyte (CTL) responses are raised (Iwasaki *et al.*, 1997).

In DNA vaccination via the skin, dendritic cells are the major APC type involved in presentation (Cella *et al.*, 1997). A particular kind of dendritic cell, the Langerhans' cell, is abundant right underneath the epidermal layer. They are able to uptake the antigen and migrate to the lymphoid organs for presentation. The antigen can be processed into peptides and presented both via MCH class I and class II. Once in the lymphoid organs, Langerhans' APC's mature and are able to deliver co-stimulatory signals crucial for T-cytotoxic and T-helper cell activation.

Very little amounts of DNA (micrograms) are sufficient for an immune response to be developed. The dose varies with the inoculation method. DNA can be administered as *'naked DNA'* or as liposomes. The most commonly used methods of inoculation are intradermal injection (i.d.), intramuscular injection (i.m.) and *'gene gun delivery'* or particle bombardment. The one used in our experiments is the gene gun, and it was very efficient in small animal studies (Fynan *et al.*, 1993). In this technique, DNA is co-precipitated with calcium chloride onto the surface of microscopic gold beads, which are later evenly deposited into the walls lining Teflon tubing. High-pressure propels the DNA-coated gold beads into the animal's skin.

Many other tissues besides skin have been tested as targets for DNA vaccination. The ideal tissue target should be easy to access and transfect. In our case, the skin was chosen since it can be readily accessed and has been successfully used as a target tissue in many other similar DNA vaccination experiments. Gene gun inoculation requires lower DNA doses than i.m. and i.d. injections, although i.m. injection requires a single dose in mice as opposed to the three doses required for gene gun inoculation (Bohm *et al.*, 1996; Hartikka *et al.*, 1996). Nevertheless, intramuscular injection is a variable technique, depending on the operator's skills, whereas the results obtained with the gene gun are repeatable and consistent. The transfection efficiency is higher when using the gene gun, since the DNA forces its entrance into the cells. The i.m. dose required in mice to raise a good immune response ranges from 50 to 100 µg, while with the gene gun, three doses of 6 µg each are sufficient.

Recently, an apparatus called '*Biojector*^{TM}' has appeared for intramuscular injections. It consists of a needleless syringe driven by CO_2 pressure. Its usage results in a more even diffusion of the DNA into the muscle tissue. Liposomes improve transfection efficiency as compared to naked DNA injection, and they can entrap plasmids, to facilitate an efficient '*in vivo*' transfection method (Gregoriadis *et al.*, 1996). Nevertheless, liposome usage is limited to injection procedures so it was not used in the present thesis.

DNA is easy to manipulate, raising the possibility of generating designer immunogens. Modifications from the original sequence are easy to produce at the DNA level. Untranslated sequences can be introduced to enhance expression. Other genetic elements can be introduced to modify the subcellular location of the encoded protein. Many reports show the utilization of immunostimulatory molecules to enhance or drive the immune response to a particular type (Xiang and Ertl, 1995; Kim *et al.*, 1997; Chow *et al.*, 1997). For allergy vaccines, it is crucial to bias the immune response towards a Th1 response, and that has been done by encoding the appropriate cytokines (IL-12, IL-18, IFN-γ and IFN-α) or chemokines in DNA vaccines (Hsu *et al.*, 1996). The presence of immunostimulatory sequences (ISS) in bacterial plasmid DNA was demonstrated long ago (Tokunaga *et al.*, 1984). These consist of CpG motifs arranged into palindromic sequences (Krieg *et al.*, 1995). ISS have been shown to induce an innate Th1 response by macrophage and B-cell activation, and by inducing type I IFN secretion. For some intracellular pathogens, such as *Listeria monocytogenes* or *Leishmania major*, CpG

motifs in DNA vaccines have been used to bias the immune response towards a Th1 response, which is much more favorable for the immune system to clear the infection (Zimmermann *et al.*, 1998; Krieg *et al.*, 1999).

It is possible to encode adjuvants in the DNA constructs either in cis or in trans. It has been proven that incorporation of genes encoding cytokines can be useful to bias the immune response towards an appropriate branch (i.e. T_{H1} or T_{H2}) (Lowry and Whalen, 1999). This is especially important for vaccines against intracellular bacterial or protozoan parasites, since a T_{H2} response would be even more detrimental to the course of an infection. Also, protein boosting can enhance the immune response after DNA vaccination, either with recombinant protein or using pseudotyped vaccinia virus.

Finally, another advantage of DNA vaccination is their safety. Vaccines based on retroviral vectors always have the possibility of pathogenesis or integration in the target cell's genome with the subsequent risk of carcinogenesis. Adenoviral vectors are less likely to produce pathogenesis, and they are not integrative, but there is usually a strong host immune response against the vector itself, hindering the effectiveness of subsequent doses. With DNA vaccines, the DNA is transfected transiently, thus the probability of non-integrative DNA molecules entering a cell, integrating randomly in the cell's genome, and activating an oncogene or inactivating a tumor suppressor, is extremely low. Some worries were raised relevant to the possibility of anti-DNA antibody induction and subsequent generation of systemic lupus erythematosus (SLE) (Gilkenson *et al.*, 1995). In that study (Gilkenson *et al.*, 1995) mice were used as a model, and dsDNA was

administered along with the Complete Freund's Adjuvant plus methylated bovine serum albumin. It is believed that these accompanying substances were determinant in raising anti-DNA antibodies. Anti-dsDNA antibodies could only be induced in mice genetically prone to autoimmune disease. Thus, this concern is not completely ruled out, but can be reasonably dismissed.

Codon Optimization

When trying to synthesize HIV proteins in mammalian systems, low levels of expression were observed (Haas *et al.*, 1996). This is believed to be due to an extreme codon bias in HIV genome. The HIV viral RNA is AU-rich, as opposed to the high GC content of the mammalian genome. The tRNAs required for viral mRNA translation are scarce in mammalian cells, and as a result of this, the viral protein levels are low (Kypr and Mrazek, 1987; Stephens *et al.*, 1999). Another factor that contributes to lowering HIV expression levels is the existence of instability sequences in the viral mRNA that require the Rev regulatory gene product for mRNA stabilization and transport to the cytoplasm (Maldarelli *et al.*, 1991; Brighty *et al.*, 1994; Kotsopoulou *et al.*, 2000). This is the main disadvantage found for DNA vaccination against HIV. Here we propose codon optimization or '*humanization*' as a means to circumvent this problem. Codon optimization will not only be more favorable on terms of tRNA availability, but since it involves many modifications in the nucleotide sequence, it will destroy the instability sequences.

In the present work, a model to prove the efficacy of codon optimization in the context of DNA vaccination is presented. If the results are positive, codon optimization will be applied to all subsequent gp120 and deglycosylated gp120 constructs.

CMV IE promoter and Intron A

The Cytomegalovirus Immediate Early (CMV IE) gene promoter and Intron A have been shown to enhance expression levels of reporter genes encoded in vectors when tested in parallel with other promoters *'in vitro'* (Pasleau *et al.*, 1985; Chapman *et al.*, 1991) and '*in vivo*' (Hartikka *et al.*, 1996; Xu *et al.*, 2001). In this thesis all three vectors carry the CMV IE promoter, since its potency is widely accepted. Intron A has been shown to cooperate with the CMV IE promoter, yielding even higher expression levels (Mikkelsen *et al.*, 1992). Also, a transcription factor binding-sequence is located in the Intron A sequence, that is thought to provide a promoter-specific regulatory element which might contribute to the enhancing effect of Intron A (Chapman *et al.*, 1991). There is direct evidence that splicing and mRNA nuclear export is coupled in higher eukaryotes (Luo *et al.*, 1999). According to this and previous studies (Huang and Gorman, 1990), the presence of an intron in a pre-mRNA increases the rate of transport into the cytoplasm. Early retroviruses, such as simian virus type D, require a cellular factor to bind an element in the RNA sequence to trigger efficient mRNA transport (Gruter *et al.*, 1998). In the case of HIV, the product of the viral gene Rev, which binds the Rev response element sequence (RRE) in the viral mRNA mediating its transport, provides this function. Thus, the deletion of the RRE would require the introduction of other elements to make up for Rev functions; an intron might be a successful candidate. According to

Chapman *et al.*, 1991, the CMV IE Intron A has transcription factor binding sites, which was corroborated by Mikkelsen *et al.*, 1992. This fact, as well as spliceability, may account for a better expression of constructs containing intron A. Here, the role of intron A is tested from an immunological point of view using the immune response generated against the encoded antigen as a reporter of this element's importance.

Tissue Plasminogen Activator Leader Sequence

The HIV-1 env signal sequence has been recently proven to delay its own cleavage, therefore slowing down the rate of gp120 folding inside the endoplasmic reticulum (Li *et al.*, 2000). Before this direct evidence was provided, substitution experiments were conducted in which the HIV leader sequence was removed and other glycoprotein leaders were inserted *in lieu* (Chapman *et al.*, 1991). A very marked increase in gp120 production was detected following substitution of HIV-1 env leader sequence with tPA leader sequence. In the present report, this effect is reflected in a higher specific-antibody production.

N-linked Glycosylation of HIV-1 gp120

The HIV-1 surface protein (gp120) is a glycoprotein. It is initially synthesized in the endoplasmic reticulum as a precursor called gp160. gp160 will yield after being processed two proteins: the surface protein, gp120, and the transmembrane protein, gp41. In some cases, an intermediate size protein – gp140 – is generated in HIV studies. gp140 contains the full gp120 (surface protein) plus the extracellular domain of gp41

(transmembrane protein). The immature gp160 protein undergoes folding and addition of complex oligosaccharides. One kind of such glycans is the N-linked oligosaccharide. Figure 1 shows a scheme of the disposition of the loops in HIV gp140, and the glycosylation sites. The functions associated with protein glycosylation are diverse, ranging from stabilization of folding intermediates, to cell-to-cell signaling. There is evidence supporting the idea that glycosylation of gp120 might actually have a role in evading the action of the immune system (Fenouillet *et al.*, 1990; Doe *et al*., 1994; Willey *et al.*, 1996; Chackerian *et al.*, 1997; Edinger *et al.*, 1997; Reitter *et al*., 1998; Mori *et al*., 2001). Other observations led to the conclusion that the first variable loop in gp120 (V1) might be especially involved in immune system evasion (Lee *et al.*, 1992; Thali *et al.*, 1993; Wyatt *et al.*, 1995, 1998; Trkola *et al.*, 1996; Wu *et al.*, 1996; Dumonceaux *et al.*, 1998; Rizzuto *et al.*, 1998, 2000; Kolchinsky *et al.*, 2001). V1 is a highly variable loop among different subspecies, and glycosylation sites on its tip are invariably present at different positions. The position of V1 changes upon interaction with the primary receptor (CD4), revealing the secondary receptor interaction site. For this reason, it is believed that glycosylation on V1 may account for an immune system evasion mechanism by which the conserved epitopes are occluded by a highly variable (i.e. neutralizing antibody resistant), highly glycosylated loop. Glycosylation on this loop might pose a physical obstacle for the antibodies to interact with the conserved epitopes underneath. Removal of the glycans on the V1 tip might make the conserved region covered by it more accessible to antibodies. In this thesis, in an attempt to reveal putative conserved epitopes occluded by N-linked glycans on gp120, several point mutations were introduced in the V1 region of gp120 from different HIV-1 subtypes.

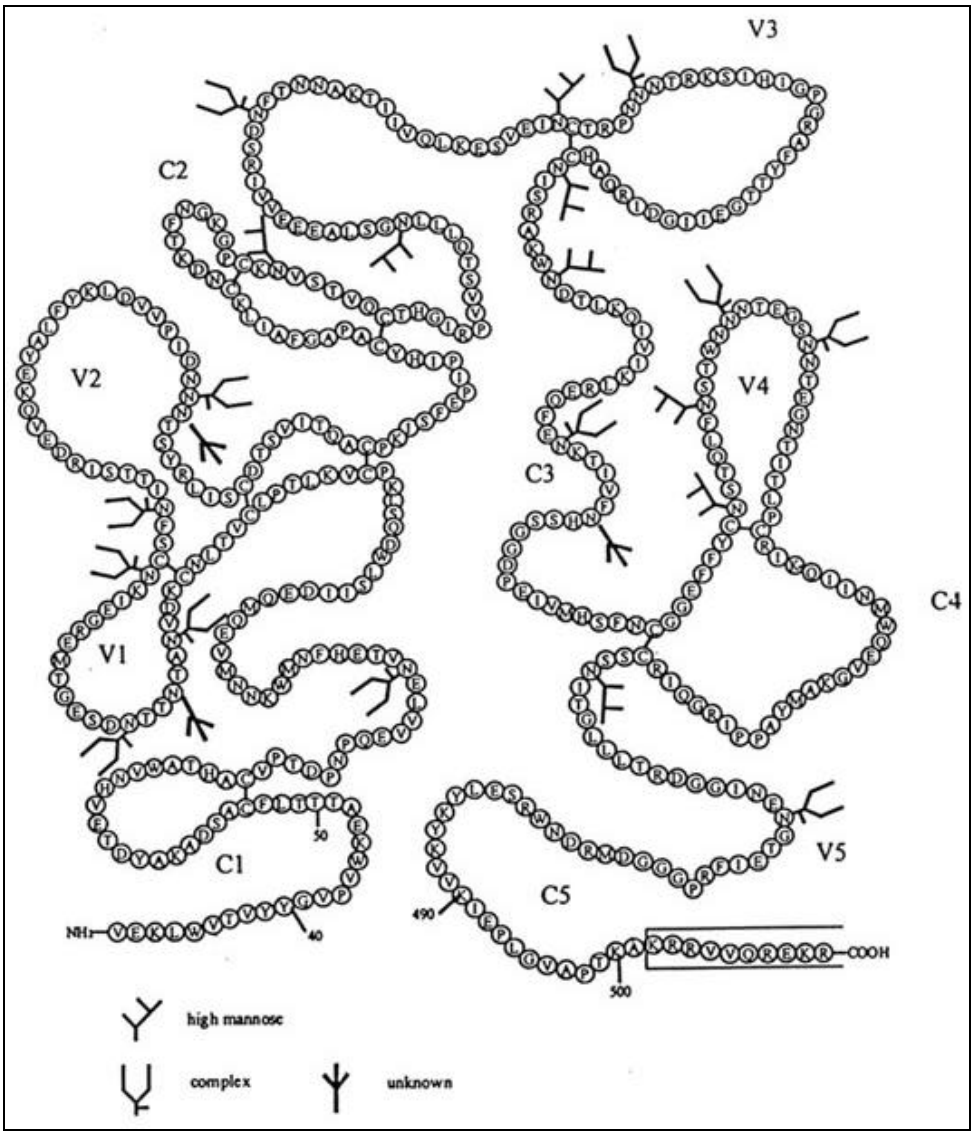

Figure 1: schematic representation of HIV-1 isolate JR-FL gp140. Note the positions of the N-linked oligosaccharides in the V1 and V2 regions. From Binley *et al.*, 2000.

Glycoproteins and Immune System Evasion

Based on several previous studies detailed below, we suspected that env protein with glycan residues removed at particular locations might expose conserved antigenic determinants without affecting the native conformation of the protein. This raised the possibility of removing those carbohydrate residues to elicit neutralizing antibody responses.

Generation of CTL responses was enhanced by deglycosylation (Doe *et al.*, 1994). In that study, gp120 was produced as fully glycosylated native protein, as a deglycosylated form, in a denatured form, and in a combination of both denatured and deglycosylated. The induction of CTL responses was more efficient when deglycosylation prior to denaturing was performed.

Some of the glycosylation sites in gp120 have been proven critical for infectivity. In the cell line-adapted HXB2 strain, 5 glycan residues were indispensable for viral replication; the remaining 19 could be removed without observing replication impediment (Lee *et al.*, 1992). The position of the oligosaccharide residues in several cell line adapted-env proteins were compared and it was observed that the relative positions were highly conserved in at least half of the sites. Single mutants were constructed, in which the Asn in a single canonical glycosylation site was substituted by Gln or His. Each mutant was tested for infectivity by syncytium formation and RT activity assays. Six mutants showed impaired infectivity as compared to the wild type virus. Mutations were also introduced at the same potential glycosylation sites, but in the third canonical

residue (Ser/Thr) rather than in the Asn. An infectivity recovery, would have been a sign that the loss of infectivity was due to the change of the Asn rather than to the lack of the glycan at that particular site. Reversion in the third site mutants was only observed in one of the six replication-impaired mutants, leaving five glycosylation sites crucial for HXB2 HIV replication (Lee *et al.*, 1992). Four of these are located in the hypervariable regions. This proved that many glycan residues are involved in functions other than infectivity; opening the possibility that glycosylation in gp120 has a role in immune evasion.

An association between viral envelope glycosylation and neutralizing antibody activity has been suggested (Willey *et al.*, 1996). In that report, the viral proteins were analyzed by radiolabelling virus-infected cells. Two types of cells were tested: peripheral blood mononuclear cells (PBMCs) and monocyte derived macrophages (MDMs). After SDS PAGE, two distinct patterns were observed in the resolution of the gp120 bands. The MDM-derived virus generated a diffuse band whereas the virus-infected PBMC-derived gp120 had a sharp appearance. This was postulated to reflect a difference in the envelope processing mechanisms in these two cell types. An analysis after endoglycanase treatment revealed a sharp appearance for the gp120 band derived from both infected cell types. Neutralization assays measuring RT activity after infection of PBMC target cells with the progeny of MDM or PBMC-infected cells, showed an eight to ten-fold difference. The MDM-derived virus was more resistant to neutralization, suggesting that the difference in the glycosylation pattern might account for this fact.

An experiment in Rhesus macaques revealed the possible importance of the glycan moieties in immune evasion (Reitter *et al*., 1998). Several mutant viruses were constructed in which point mutations were introduced to change the canonical N-linked glycosylation sequences (Asn to Gln) in the V1 loop. Viral loads in the monkeys infected with these mutant SIVs were dramatically reduced until the 12th week post-inoculation, in some of them up to the 56th week. The sera were analyzed for ELISA reactivity against V1 peptides. Titers were extremely high compared to those obtained with sera from monkeys inoculated with the parental virus. The effect occurred both against deglycosylated and wild type V1 peptides. Neutralization activity at serum dilution higher than 1:1000 was observed against the parental SIV with some antisera collected from the deglycosylated mutants. More interestingly, the analysis of the viral progeny revealed restoration of the glycosylation, not in the exact same sites, but in their vicinity. The percentage variation of the progeny's genome sequence from the sequence of the virus inoculated showed a significant increase as compared to the wild type-infected monkeys. This clearly reflects an adaptation of the virus to the immune selective pressure exerted by the neutralizing antibodies raised against the conserved domains exposed after deglycosylation. In this case, the antibody production was measured against a V1 peptide, instead of the whole wild-type gp120. Neutralization was also achieved, but it is not known whether the neutralizing antibodies were raised against epitopes in V1 itself or against the conserved core domain mentioned in the structural studies described above. For this reason, it would be interesting to test cross-neutralization, i.e. to check whether neutralization occurs also against divergent isolates, that would support the hypothesis of a conserved epitope being exposed by deglycosylation.

Some residues in V1 are candidates for deglycosylation, since this loop has been known to occlude conserved regions critical for viral entrance. It has been postulated that the first two variable loops on HIV-1 gp120 are covering a core structure on gp120 (Wyatt *et al.*, 1995; Trkola *et al.*, 1996; Wu *et al.*, 1996), that would be exposed upon gp120 interaction with CD4. This hypothesis has been further confirmed by X-ray crystallography analysis of gp120-soluble CD4 complexes (Wyatt *et al.*, 1998). It was also noted that those newly exposed protein domains are conserved epitopes that can be recognized by monoclonal antibodies (Thali *et al.*, 1993; Cao *et al.*, 1996; Wyatt *et al.*, 1998). The ability of gp120 – through its V3 loop – to interact with the co-receptor (CCR5 or CXCR4) is influenced by a conserved domain located in the core structure of gp120 (Rizzuto *et al.*, 1998, 2000). Some HIV-2 (Endres *et al.*, 1994) and SIV (Edinger *et al.*, 1997) isolates are known to be able to infect target cells independently from CD4. The same CD4-independent infections have been achieved with HIV-1, after in vitro passage in CD4-negative cells (Dumonceaux *et al.*, 1998). All this taken together leads to the suggestion that the requirement of CD4 binding to gp120 and further exposure of the conserved core domain that interacts with the co-receptor may actually be a mechanism of immune evasion, where the outer surface of gp120 is highly variable, but only upon interaction with CD4, is a conserved domain crucial for viral fusion with the cell revealed. Attempts have been made to expose these conserved epitopes. In one of them (Lu *et al.*, 1998), the increase in HIV-1 env immunogenicity was tested after deletions in the V1/2 and V3 regions were introduced. The three forms of env (gp160, gp140 and gp120) were subject to this deletion. Dr. Lu and co-workers used the DNA vaccine

approach to construct mutant plasmids with these deletions, then test for ELISA and neutralization antibody production in rabbits. The constructs carrying the deletions showed an increase in the immunogenicity for gp140 while the immunogenicity was decreased for the gp120 V1/2V3-deleted constructs. Apparently, the deletion caused the creation of new epitopes as well as the loss of others. The neutralization was not improved in any case, which might suggest that the deletions in V1/2V3 caused a significant rearrangement of the protein, and the newly exposed epitopes were different from the ones discussed above. In another study (Kolchinsky *et al.*, 2001), an attempt was made to expose the conserved epitopes in the gp120 core. This time another kind of mutation was introduced: based on previous findings of the possible role of glycans in occlusion of conserved epitopes, mutated constructs were analyzed in which the canonical N-linked glycosylation sequence was mutated at different positions in V1/V2. The results indicate that some of the mutated viruses were CD4-independent for infection. Data for co-receptor binding as well as for an infectivity assay were provided, as well as a structural model in which an Asparagine-linked oligosaccharide in V1/V2 appears blocking the gp120-CCR5 interaction site.

Very recently a mutant strain of SIVmac239, with five glycan residues removed at the V1/V2 region, has been reported to induce almost complete protection from wild type SIVmac239, without any reversions to the glycosylated phenotype being observed (Mori *et al.*, 2001). Infection with the mutant resulted in the same viral replication pattern as with the wild-type, peaking at 4 weeks after infection, but the chronic pattern typical of SIV (and HIV) infection was not observed for the mutant-infected monkeys.

Furthermore, these monkeys were able to withstand a challenge with the wild-type virus, which resulted in a low replication levels and low chronic infection instead of the typical chronic infection pattern. In different stages the researchers were able to amplify proviral DNA, and the five deglycosylation mutations remained the same. Surprisingly, analysis of the neutralizing activity of the monkey sera revealed low neutralization titers. In other studies a low neutralizing antibody response was always observed, usually accompanied by high CTL responses (Johnson and Desroisiers, 1998). The authors raised the possibility that glycosylation in gp120 might have a role in protection from proteolysis prior to antigen presentation. This should be reflected in the CTL assays, but when the CTL responses were tested, in most cases they were very similar both in mutant-infected monkeys and in wild type-infected. Nevertheless, the CTL responses appeared earlier after challenge in the mutant infected monkeys than in the naïve ones, suggesting that the low level of mutant virus replication in the chronic phase may have contributed to maintaining a high number of memory cells.

STATEMENT OF THESIS

The first hypothesis tested in this thesis is that use of specific controlling elements in DNA vaccines will increase immunogenicity. An optimized vector will be used. The vector includes the Cytomegalovirus immediate early (CMV IE) promoter along with the CMV IE gene Intron A, and the tissue plasminogen activator (tPA) leader sequence replaces the HIV leader sequence. I postulate that this vector will yield better expression levels *'in vitro'* and *'in vivo'* — as reflected by the specific antibody production against the antigen encoded in the vaccine.

The second hypothesis tested in this thesis is that codon optimization towards a mammalian bias of the gp120 sequence will enhance the immunogenicity due to increased protein expression levels from the DNA vaccine construct.

The third hypothesis tested in this thesis is that directed mutagenesis in the DNA sequence of the HIV-1 gp120 V1 region will lead to the expression of partially non-glycosylated antigens, thus creating a candidate for an engineered DNA vaccine against HIV-1.

EXPERIMENTAL APPROACH

A successful DNA vaccine will require high levels of antigen expression. Codon optimization is meant to enhance protein synthesis in heterologous systems and to increase mRNA stability. HIV codon bias is distant from mammalian, which hinders expression levels in a mammalian system. Using chemical synthesis, it is possible to generate a DNA sequence encoding the same amino acid sequence as HIV gp120 but with a codon usage more similar to the well-characterized mammalian codon bias. The postulated increase in expression levels will expectedly yield higher antibody titers and better cell mediated immunity.

In this thesis several sequence modifications have been devised to increase gp 120 immunogenicity. Deglycosylation will be performed at particular sites on the gp120 V1 loop in an attempt to create a DNA vaccine yielding an antigen with exposed conserved antigenic determinants. Some of the glycan moieties in gp120 are suspected of occluding conserved protein domains in an attempt to evade the immune system. Using directed mutagenesis, constructs will be made in which N-linked glycosylation sites are selectively removed without altering the conformation of gp120. This thesis will cover the production of the DNA vaccines, its administration to animal subjects, and characterization of the protein expressed '*in vitro*'.

MATERIALS AND METHODS

Recombinant DNA techniques

Polymerase Chain Reactions

PCR reactions were performed using a MJ Research PTC-150 Minicycler™ Thermocycler. Annealing temperatures for the primers were determined using Mac Vector software package, and were variable for the different reactions. Pfu polymerase was used for high fidelity amplification. After the reactions were complete, the PCR products were purified using the QIAquick™ PCR purification kit (see manufacturer's manual for details).

Plasmid DNA purification

LB-Amp broth was inoculated with the desired culture and incubated overnight at 37°C. Plasmid DNA was then extracted from the cultures using the Clontech Nucleospin™ Mini-prep kit (see manufacturer's manual for details). DNA was eluted from the columns in 50 µl of TE buffer or in distilled water if the next reaction was salt-sensitive.

Agarose Gel Electrophoresis

Agarose was dissolved in TAE buffer to a 1% (w/v) concentration. The mixture was then heated in a microwave oven until the agarose was completely dissolved. A Bio-Rad agarose gel casting system was used to pour the gel and after the agarose cooled down, samples were loaded with 4X loading buffer. The gel was run in a Bio-Rad gel box at approximately 50-70 Volts for one and a half to two hours. After that, the gel was stained in an Ethidium Bromide solution (25 ng/ml in TAE buffer) for 20-30 min. The stained gel was then de-stained in TAE buffer for 20 min and a photograph was taken using a Kodak DC-40^{TM} digital camera under UV light.

Restriction Endonuclease Digestion

The final volume for restriction enzyme digestions was 10 µl for analytical digestions and 30 µl for preparative digestions. The appropriate enzyme concentration and buffer, BSA, DTT, and DNA concentrations were estimated according to the New England BioLabs catalogue.

Restriction Fragment Purification

After running an agarose gel, targeted DNA bands were cut and purified from the gel using the QIAquick^{TM} gel extraction kit (see manufacturer's manual for details).

Ligation

Appropriate amounts of prepared insert and vector were estimated from an agarose gel and added to a ligation reaction mix containing T_4 ligase and ligase buffer in the amounts indicated in the Rôche catalogue. The reactions were run overnight at 16°C.

Transformation

E. coli HB101 competent cells were stored at -70°C, 100 µl/vial. The vial was thawed on ice. A certain amount of plasmid DNA or ligation mixture was added to the vial and mixed gently. The mixture was then incubated on ice for 30 min. Without mixing, the tube was removed and placed in a water bath at 42°C for 90 seconds. 400 µl of LB broth were added to each tube and incubated at 37°C for 45 min. After the incubation period, 100 and 300 µl of the transformation mixture were spread on different LB-Kan plates and they were allowed to incubate at 37°C overnight. The following day, colonies were picked for mini-prep analysis.

SDS PAGE and Western Blots

A 12 % Acrylamide/bis-acrylamide minigel was run with the supernatant and or lysate obtained from harvesting the transfected 293T cells, for approximately 2 hours at 50 mA. Using a semi-dry blotting apparatus, the protein was transferred to a PVDF membrane for 1.5 to 2 hours at aproximately 80 mA per gel. The cut piece(s) of membrane were pre-treated by submerging it into methanol for 2 min, then it was transferred to ddH_2O and washed, and finally it was soaked in transfer buffer. A cut piece

of 3MM Whatman™ paper (soaked in transfer buffer) was placed on the anode of the blotting apparatus then the membrane, then the gel, then another piece of Whatman™ paper. After the transfer was done, the membrane was incubated overnight in 15 ml of blocking solution (PBS, Tween-20 0.1-0.2% v/v, I-Block™ 0.1% w/v) at 4° C.

Antibody stocks were diluted to the desired concentration (1:200 for rabbit sera) in blocking solution. 5 ml of the diluted antibody were added to each membrane and it was allowed to incubate for 1 hour on the rotator at low speed. The membrane was then washed four times, 20 min each, with 15 ml of blocking solution, on the rotator at vigorous speed. The membrane was then incubated with the secondary antibody solution (diluted 1:5000 in blocking solution) for 1 hour, on the rotator at low speed. The membrane was then washed four times, 20 min each, with 15 ml of blocking solution, on the rotator at vigorous speed.

Chemiluminescence was performed using the Tropix Western Light™ protein detection kit. Two pieces of thin, transparent plastic, big enough to cover the membrane were cut. 1.5 ml of substrate was added per membrane. The “sandwich” was allowed to incubate for 5 min. The membrane was dried on a paper towel, and transferred to a new dry sandwich. This was exposed in the darkroom for variable times.

DNA Tubing Preparation

For all the procedures in this section, a Bio-Rad tubing prep station was used. Rislan tubing was dried for 1–2 hours by forcing N_2 at ~ 0.2 L/min into the tubing. The ends of the tubing were capped after drying to keep moisture out. Water was added to 1 µm gold beads (adjusted for each experiment) to achieve a final concentration of 100 mg/ml. The gold beads were centrifuged to the bottom of a microcentrifuge tube for ~10 seconds and the water was removed with a pipette, leaving a small amount of water (~50 µl) in the tube. A 100 µl aliquot of spermidine (100 mg/ml in water) was added to the gold bead pellet, and the mixture was vortexed thoroughly at high speed until the gold was completely resuspended. Plasmid DNA was added to the beads/spermidine suspension. The mixture was vortexed only briefly on high, as the DNA can shear easily. $CaCl_2$ (2.5 M in water) was added drop-by-drop into the mixture while vortexing at medium speed. The mixture was let stand at room temperature for 3-5 minutes to allow precipitation, and then centrifuged for 8 seconds, decanted and the supernatant was discarded. The coated gold beads were washed 5 times with 1ml dehydrated absolute ethanol. Each time, the ethanol-resuspended beads were centrifuged for 8-12 seconds and the supernatant removed. The beads were resuspended in the total volume of absolute ethanol needed for each preparation in a 20 ml glass scintillation vial and capped tightly. A piece of tubing 2 –3 inches beyond the right end of the tubing prep station was cut. A 10 ml syringe was attached to the right end of the cut tubing. The glass vial of gold beads was sonicated briefly to completely suspend the beads, and the suspension was drawn into the tubing with a syringe. The gold was allowed to settle out of the suspension in the tubing for 10 minutes. Then the ethanol was slowly drawn from the tubing with the

syringe at a rate of about 2 inches per second. The tubing was connected to the nitrogen port and the prep station was turned on to rotate the tubing and spread the gold over the inside of the tubing for 1 minute. The nitrogen flow was turned on to 0.4 L/min to dry the remaining ethanol from the tubing for 5 minutes as it continued to rotate. The tubing was cut into half-inch cartridges using the tubing cutter, sealed in a scintillation vial with parafilm, and stored at -20^{o}C.

Animal Groups for Immunization

Rabbits

New Zealand white syngenic rabbits were used to test the effect of deglycosylation on gp120 immunogenicity.

Table I: Animal Groups and Immunizations Administered for the Rabbit Experiment. The table shows the composition of the vaccine formulation used to inoculate the rabbits in each group. dG: deglycosylated.

Groups	Rabbit #	gp120 DNA vaccines	rgp120 protein
Group 11	C11-1,2	B	B
Group 12	C12-1,2	B/dG1	B/dG1
Group 13	C13-1,2	Bal/dG1	Bal/dG1
Group 14	C14-1,2	Czm	Czm
Group 15	C15-1,2	Czm/dG1	Czm/dG1
Group 16	C16-1,2	E/dG1	E/dG1
Group 17	C17-1,2	B, Bal, Czm, E	B, Bal, Czm, E
Group 18	C18-1,2	(B, Bal, Czm, E)/dG1	(B, Bal, Czm, E)/dG1
Group 19	C19-1,2	(A2, B, Czm, D, E, F, G, Ba-l)/dG1	(B, Bal, Czm, E)/dG1
Group 20	C20-1,2	(A2, B, Czm, D, E, F, G, Ba-l)/dG1	(DNA boost)
Group 21	C21-1,2	vector	(B, Bal, Czm, E)/dG1

Table II: Immunization, bleeding and protein booster schedule for the rabbit experiment.

Immunization Shedule												
DNA vaccine	I	II	III			IV						
Bleed	I	II	III	IV	V	VI	VII	VIII	IX	X	XI	XII
Protein Boost								I		II		
Week	1	5	9	11	15	19	21	23	25	27	29	31

Mice

BALB/C syngenic mice were used to test the effect of codon optimization, intron A and leader sequence on gp120 expression levels.

Table III: Animal groups for the mouse experiment. pJW4303 contains Intron A while pCMV12 does not. hiv represents HIV leader and tPA represents tPA leader. HXB2 is the lab-adapted strain gp120. Syn is the codon-optimized gp120 based on the JR-FL sequence.

Groups	DNA Vaccine	mg DNA/animal	No. of animals
A	Vector 1	6	4
B	Vector 2	6	4
C	Intron A hiv.gp120.HXB2	6	4
D	Intron A tPA.gp120.HXB2	6	4
E	Intron A hiv.gp120.syn	6	4
F	Intron A tPA.gp120.syn	6	4
G	hiv.gp120.HXB2	6	4
H	tPA.gp120.HXB2	6	4
I	hiv.gp120.syn	6	4
J	tPA.gp120.syn	6	4

Table IV: Immunization and bleeding schedule for the mouse experiment.

Immunization Shedule							
DNA vaccine	I	II	III				
Bleed	I	II	III	IV	V	VI	VII
Week	1	5	9	11	13	17	21

Anesthesia, Immunization and Bleeding

Rabbits

A portion of skin was cleaned for the injection of anesthetic solution into the right hind leg quadriceps or lumbar muscle of each animal. The anesthetic solution consisted of Ketamine (100 mg/ml)/Xylazine (100 mg/ml)/saline. The total volume of the anesthetic solution each animal received was calculated based on the animal's weight (see table V). Rabbits were then bled from the central ear vein. The backside of the ear was rubbed briskly with an alcohol prep. Then, using a 23-gauge butterfly needle, blood was removed with a syringe until the desired amount was collected. The blood was then transferred to a vacuum tube. The animal's abdomen was then shaved, and DNA-coated gold beads were inoculated to the shaved surface using the gene gun. Each animal received 36 μg of DNA per dose, and four doses were administered according to the schedule in table II.

Table V: Dose and composition of the anesthetic solution injected to the rabbits

		Dosage/animal (mg)	
Weight of rabbit (Kg)	Dose of mixed Ket/Xyl (ml)	Ketamine	Xylazine
2.0-2.5	0.60	50.0	10.0
2.5-3.0	0.65	54.2	10.8
3.0-3.5	0.70	58.3	11.7
3.5-4.0	0.75	62.5	12.5
4.0-4.5	0.80	66.7	13.3
4.5-5.0	0.90	75.0	15.0
5.0 & up	1.00	83.3	16.7

Mice

The abdominal fascia was rubbed with an alcohol prep, and 0.5-0.7 µl of anesthetic solution (Ketamine (100 mg/ml)/Xylazine (100 mg/ml)/Saline 4:1:10) was injected intraperitoneally using a tuberculin syringe. Once the animals were sedated, a glass capillary was used to draw blood from the periorbital cavity. The abdominal area was then shaved, and DNA-coated gold beads were inoculated using the gene gun. Each animal received 3 doses of 6 shots each according to the schedule in table IV.

ELISAs

Concanavalin A Antigen Capture ELISA for Quantification of gp120

96-well flat bottom plates were coated with 100 µl/well of Concanavalin A (ConA) at a concentration of 50 µg/ml in PBS, pH 7.4 and incubated for 1 hour at room temperature (RT). The plates were washed with wash buffer (PBS/0.1% Triton X-100) 5 times: 3 times for 1 min, once for 5 min, and once for 15 min. 100 µl/well of PBS diluted gp120 antigen were added in duplicate, serial dilutions were performed, and the plates were allowed to incubate for 1 hour at room temperature (RT). After that the plates were washed as above. Free ConA binding sites were blocked with 200 µl/well of blocking buffer, and incubated for 1 hour at RT. The plates were washed as above. 100 µl of anti-gp120 rabbit sera at 1:5000 dilution in whey dilution buffer (PBS/4% whey/0.5% Tween-20) were added to each well and allowed to incubate for 1 hour at RT. The plates were washed as before. 100 µl of biotinylated anti-rabbit IgG at 1:1000 in whey dilution buffer were added to each well and allowed to incubate for 1 hour at RT. The plates were washed again. 100 µl of streptavidin-conjugated horseradish peroxidase (HRP-streptavidin) at 1:2000 in whey dilution buffer were added to each well, and allowed to incubate for 1 hour at RT. The plates were washed as above. Fresh TMB substrate (1 TMB tablet/0.05 M phosphate/citrate buffer/0.006% H_2O_2) was prepared, and 100 µl were added to each well allowing 3.5 min incubation time at RT. The reaction was stopped by adding 25 µl of 2M H_2SO_4 to each well, and the OD was read at 450 nm using a Dynex Opsys MR^{TM} plate reader.

With this assay (the Antigen Capture ELISA for Quantification of gp120) the antigen concentration was normalized, using a serum raised by polyvalent gp120 immunization, to give an equal concentration.

Concanavalin A Antigen Capture ELISA for Detection of Antibody

96-well flat bottom plates were coated with 100 µl/well of Concanavalin A at a concentration of 50 µg/ml in PBS, pH 7.4 and incubated for 1 hour at room temperature (RT). The plates were washed with wash buffer 5 times: 3 times for 1 min, once for 5 min, and once for 15 min. 100 µl/well of PBS diluted normalized gp120 antigen (concentration normalized with the Antigen Capture ELISA for Quantification of gp120) at around 1 ug/ml were added and allowed to incubate for 1 hour at room temperature. After that the plates were washed as above. Free ConA binding sites were blocked with 200 µl/well of blocking buffer (5% non-fat dry milk in whey dilution buffer) and incubated for 1 hour at RT. The plates were washed as above. 100 µl of anti-gp120 rabbit sera at 1:5000 dilution in whey dilution buffer were added to the wells, serial dilutions were performed, and the plates were allowed to incubate for 1 hour at RT. The plates were washed as before. 100 µl of biotinylated anti-rabbit IgG at 1:1000 in whey dilution buffer were added to each well and allowed to incubate for 1 hour at RT. The plates were washed again. 100 µl of streptavidin-conjugated horseradish peroxidase (HRP-streptavidin) at 1:2000 in whey dilution buffer were added to each well and allowed to incubate for 1 hour at RT. The plates were washed as above. Fresh TMB (1 TMB tablet/0.05 M phosphate/citrate buffer/0.006% H_2O_2) substrate was prepared and 100 µl were added to each well allowing 3.5 min incubation time at RT. The reaction was

stopped by adding 25 µl of 2M H_2SO_4 to each well and the OD was read at 450 nm using a Dynex Opsys MR^{TM} plate reader.

Setup of Murine Splenocytes for Cell Mediated Immune Response Assays

Mice were anesthetized and then euthanized by cervical dislocation. The abdominal fascia was flooded with 70% ethanol, then a transversal 1 cm midline incision was made and torn open. The spleen was then removed and placed in ~10 ml of medium (RPMI 1640 complete 10% heat-inactivated FBS 1% Penicillin-Streptomycin). The spleen-containing media was placed over a sterile platinum screen tissue sieve with a petri dish underneath, and the spleens were pressed through the screen using a sterile spatula. The homogenate was then pipetted into a 50 ml conical tube. 10 more ml of media were used to rinse the petri dish, and the suspension was added to the same tube. The tube was then centrifuged at 1,500 rpm, and the supernatant removed. The pellet was washed with 10 ml of media. Media was removed and the pellet was resuspended in 8 ml of ACK lysis buffer (NH_4Cl 16.58 g, $KHCO_3$ 2 g, EDTA-Na_2 14.4 mg, dH_2O 200 ml). This was allowed to stand for 2-3 min and spun down at 1,500 rpm. The supernatant was removed and the pellet was washed twice with 20 ml media. The supernatant was removed and a final aliquot of 10 ml of media was used to resuspend the pellet and clumps were removed. Viable cells were counted under the microscope. The cell suspension was diluted with media to a stock concentration of $5x10^6$ cells/ml.

ELISPOT Assay for Detection of IFN-g Production by Murine Splenocytes

Plates (96 well multiscreen Immobilon-P-membrane sterile white plate, Millipore) were coated overnight at 4°C with 100 µl/well capture antibody (purified rat anti-mouse IFN-γ: Rat IgG1, clone R4-6A2 PharMingen 1mg/ml) at a final concentration of 5 µg/ml in PBS. The plates were then rinsed thrice with sterile PBS, and then blocked with 200 µl/well complete RPMI 1640 (10% heat inactivated FBS 1% Penicillin-Streptomycin) for two hours at 37°C. The different peptides used for stimulation were mixed with an appropriate splenocyte amount for each of the mouse groups to a final peptide concentration of 4 µg/ml, and cell concentrations of 0.5 $x10^6$ and $0.1x10^6$ cells/ml. Con A (50 µg/ml in PBS) was used as a positive control instead of peptide, at a final concentration of 2 µg/ml. A volume of 100 µl of the splenocyte suspension mixed with peptide or ConA was added to each well. Plates were incubated 24 hours at 37°C and then rinsed twice with sterile distilled water. Plates were washed 6 times with PBS/0.05% Tween 20. Detection antibody (Biotin-conjugated rat anti-mouse IFN-γ: Rat IgG1, clone XMG1.2 PharMingen 0.5mg/ml) was diluted to a final concentration of 1.25 µg/ml in PBS/0.005% Tween 20/5% FBS and 100µl were added to each well. Plates were incubated overnight at 4°C. Plates were washed six times with PBS/0.05% Tween 20. Alkaline peroxidase-conjugated Streptavidin (AP-conjugated streptavidin, PharMingen) was diluted 1:800 in PBS/0.005% Tween 20/5% FBS, and 100 µl were added to each well and then allowed to incubate at 37°C for 30 min. The plates were washed 8 times with PBS/0.05% Tween 20. 100 µl of pre-filtered substrate (AP Substrate 1-STEP NBT/BCIP, PIERCE) were added to each well and the plates were allowed to incubate at

room temperature for 6-8 min, and then washed thoroughly under tap water and allowed to air-dry completely. Dark-blue spots were counted under a dissecting microscope and the results recorded.

Molecular Cloning of Vaccine Constructs

Deglycosylated Vaccine Constructs

For the deglycosylated constructs, the appropriate inserts were amplified by PCR from plasmids containing the gp140 gene for every clade (Gao *et al.*, 1996), and subcloned into pSW3891 vector (figure 2). Mutagenic primers were used in which mismatches were introduced creating Glutamine to Asparagine substitutions. New restriction sites were also generated to facilitate screening by introducing mismatches in the same primers (table VII). Analytic digestions were performed to check for the correct insertion (see figure 5).

The animals were vaccinated with constructs encoding the mutant form of gp120. There are several potential N-linked glycosylation sites, i.e. sites where the canonical N-linked glycosylation sequence is found (N-X-S/T). Mutations were introduced at some of these sites by changing the Asparagine residue to Glutamine, a residue similar to Asparagine in biochemical properties, but that cannot be glycosylated. These mutations targeted the tips of the V1 loop, the region that is believed to be most important in epitope occlusion. Table VI shows the positions in the gp120 V1 region that were subjected to the deglycosylation mutations.

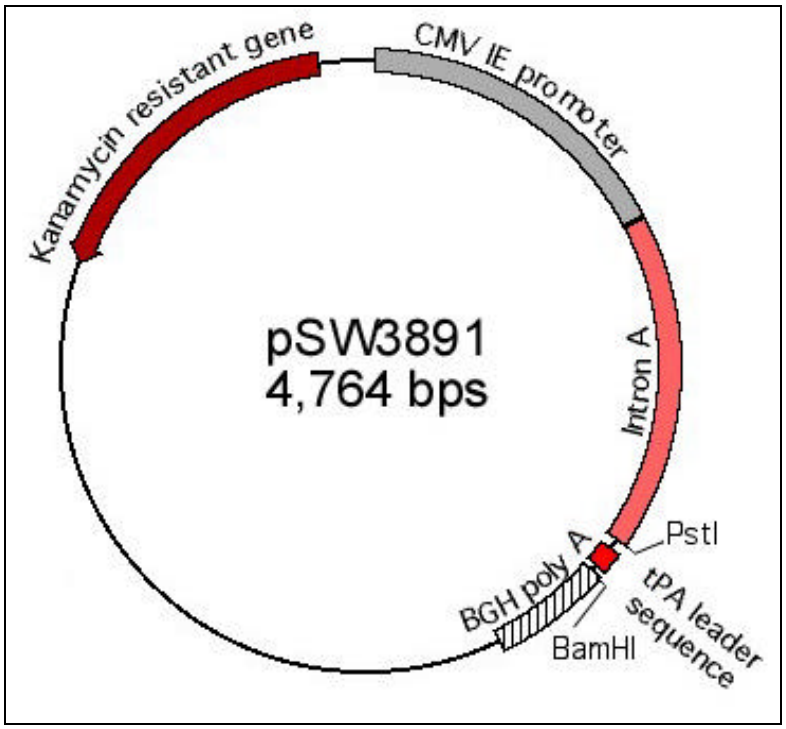

Figure 2: Vector pSW3891. Note the presence of the CMV IE promoter, Intron A, tPA leader sequence, and Bovine Growth Hormone Polyadenylation signal (BGH)

Table VI: Different deglycosylated constructs generated by directed mutagenesis. The table shows the relative positions of the V1 loop for each clade, the potential glycosylation sites in V1 and the glycosylation sites that were actually mutated.

Construct Name	Vector	Insert	V1 Loop Position in env	No. of aa in V1 loop	Potential N-linked Glycosylation sites in V1 Region	N ® Q Mutations in the Modified Constructs
pSW3891/gp120.A_2/dG	pSW3891	HIV-1 gp120 A2	128-153	24	N131, 135, 142, 152	N131, 134, 141
pSW3891/gp120.Bal/dG	pSW3891	HIV-1 gp120 Bal	130-160	29	N129, 135, 140, 143, 159	N135, 140, 143
pSW3891/gp120.B/dG	pSW3891	HIV-1 gp120 B	128-159	30	N127, 133, 136, 140, 143, 158	N133, 136, 140
pSW3891/gp120.C_1/dG	pSW3891	HIV-1 gp120 C_1	128-149	20	N130, 137, 148	N130, 137
pSW3891/gp120.C_{ZM}/dG	pSW3891	HIV-1 gp120 C_{ZM}	128-156	28	N132, 138, 143, 144, 149	N143, 144, 149
pSW3891/gp120.D/dG	pSW3891	HIV-1 gp120 D	128-147	20	N127, 132, 136, 146	N132, 136
pSW3891/gp120.E/dG	pSW3891	HIV-1 gp120 E	135-161	25	N134, 137, 142, 146, 153, 160	N137, 142, 146
pSW3891/gp120.F/dG	pSW3891	HIV-1 gp120 F	128-156	27	N134, 137, 143, 155	N134, 137, 143
pSW3891/gp120.G/dG	pSW3891	HIV-1 gp120 G	128-152	23	N130, 134, 140, 151	N130, 134, 140

Table VII: Mutagenic primers used to introduce deglycosylation mutations in gp120. Characters in italics denote changes from the original sequence. Characters in bold case represent the mutations in the Asparagine residues changing to Glutamine. Paired primers were GP120-p-B1 for the forward primers and GP120-p-F1 for the backward primers (see text below).

Clade	Primer name	Position	Sequence
A2 (92UG037)	GP120-19; Forward	405-436	AAT ATC AC*G* AAT *TCT* ATC ACC ***CAG*** AGC TCA G EcoR I
	GP120-20; Backward	422-388	GAT G*GA* ATT *C*GT GAT ***CTG*** ATT GGT GAT ***CTG*** ATA GC EcoR I
B (92US715.6)	GP120-3; Forward	438-461	gg *ACT* AGT AGT GAG ACA ATG ATG GAG GAG SpeI
	GP120-4; Backward	436-402	gg *ACTA* GT GGT CTG AGT AGC CTG CCT CGT GGT CTG AGT ATC SpeI
Bal	GP120-17; Forward	774-810	AAT GCT ACT AAT GG*C* ***CAG*** GAC ACT ***CAG*** ACC ACT AG Msc I
	GP120-18; Backward	800-765	ATT AGT GTC ***CTG*** *G*CC ATT AGT AGC ***CTG*** CCT CAA ATC Msc I
C1 (92BR025)	GP120-9; Forward	375-418	ACG TTA CAC TGC AGT ***CAG*** AGA ACT ATT GAC TAC AAT *CAG* AGA AC Pst I
C (ZM651)	GP120-27; Forward	337-371	***CAG*** ***CAG*** ACC ACC AAC GTG ***CAG*** AAC AGC ATG AAC GG
	GP120-28; Backward	336-307	CAC CAC GCT GTT ***CTG*** CAC GTT GCG GGT CAC
D (92UG021)	GP120-21; Forward	393-428	TGG AAG ***CAG*** GCC *TC*T ACT ***CAG*** GCC ACT AAT GAG GGC Stu I
	GP120-22; Backward	416-383	GGC ATT AGT GG*A* GGC ***CTG*** CTT CCA TTC AGT GCA G Stu I
E (93TH976)	GP120-13; Forward	411-449	AAT TTG ACC AAT GGC ***CAG*** AAG ACA ACT ***CAG*** GTC TCT AAC Msc I
	GP120-14; Backward	437-395	AGT TGT CTT ***CTG*** GCC ATT GGT CAA ***CTG*** GGT ACA AAT C Msc I
F (93BR020)	GP120-15; Forward	405-438	GGC ACC AAT GAC AC*G* AT*C* GCC ACC ***CAG*** GAC AGC C Pvu I
	GP120-16; Backward	434-396	GTC TTA GGT GGC *G*AT *C*GT GTC ***CTG*** GGT GCC ***CTG*** GGT GGC Pvu I
G (92UG975)	GP120-11; Forward	402-434	*CAG* TAT ACT GA*G CTC* GCT ***CAG*** ACA AGC ATT GGG Sac I
	GP120-12; Backward	425-383	TGT GTT AGC *GAG CTC* AGT ATA ***CTG*** GTT GGT TAC ***CTG*** AGC ACA G Sac I

For all the reactions, forward primers were used in combination with the GP120-p-B1 primer, which hybridizes in the 5' region of the gp140 template plasmids. Backward primers were used with the GP120-p-F1 primer, which hybridizes in the 3' region of the gp140 template plasmids.

The deglycosylated constructs prepared in this thesis were the ones corresponding to clades A_2 and G; different researchers at the Laboratory of Nucleic Acid Vaccines prepared the rest.

Cloning of the gp120.A_2 deglycosylated form was performed as follows: the vector pSW3891 was digested with Bam HI, purified with the QIAGEN PCR purification kit, and then digested again with Pst I. After another round of purification, Calf Intestinal Phosphatase (CIP) treatment was performed, and the vector was purified a final time. For the insert, two PCR rounds were performed, using as a template the wild-type gp120 form of the respective clade in the pJW4303 vector. Each of the reactions used a mutagenic primer (see list above) and a paired primer hybridizing with the pJW4303 vector sequences flanking the wild-type gp140 insert. The 5' PCR product (obtained with the first mutagenic primer and the GP120-P-B1) was digested with Eco RI and Pst I. The 3' PCR product (obtained with the second mutagenic primer and the GP120-P-F1) was digested with Eco RI and Bam HI.

Cloning of the deglycosylated gp120.G form was performed in a similar way: the vector pSW3891 was digested with Bam HI, purified, and then digested with Pst I and purified again. CIP treatment was performed, and the digested vector was purified a final time. For the insert, two PCR rounds were performed, using as a template the wild-type gp120 form of the respective clade in the pJW4303 vector. Each of the reactions used a mutagenic primer (see list above) and a paired primer hybridizing with the pJW4303 vector sequences flanking the wild-type gp140 insert. The 5' PCR product (obtained with

the first mutagenic primer and the GP120-P-B1) was digested with Sac I and Pst I. The 3' PCR product (obtained with the second mutagenic primer and the GP120-P-F1) was digested with Sac I and Bam HI. After purification, an analytic gel was run to estimate the insert and vector concentrations and the ligation reaction was set up. The next day, the ligation mixture was used to transform competent cells, which were spread on Kan agar plates and the transformants screened.

This cloning strategy provides directionality as well as the introduction of a unique restriction site in the insert, making it easier to check for the correct clones through analytic digestions of the transformants obtained.

Vaccine Constructs Used in the Mouse Experiment

The clones used in the mouse experiment were obtained from Allison Hirsh (UMass Medical School). In figure 3, the construct arrangement is shown. The vectors used had no leader sequence, and the CMV IE promoter was present with or without intron A. The leader sequence cloned upstream the gp120 gene was either the HIV leader or the tPA leader. The amino acid sequence of each of the leader sequences used is shown in table VIII. The inserts were cloned into the vector's Hind III and Bam HI sites downstream from the CMV IE promoter and upstream from the BGH poly A site.

Table VIII: amino acid sequences of the signal peptides encoded in the constructs. Positively charged amino acids are shown in bold case.

Signal Peptide	Sequence
Tissue Plasminogen Activator	MDAM**KR**GLCCVLLLCGAVFVS
HIV-1 env	**R**S**K**LM**R**V**K**E**K**YQHLW **R**WGW**R**WGTMLLGMLMICASGA

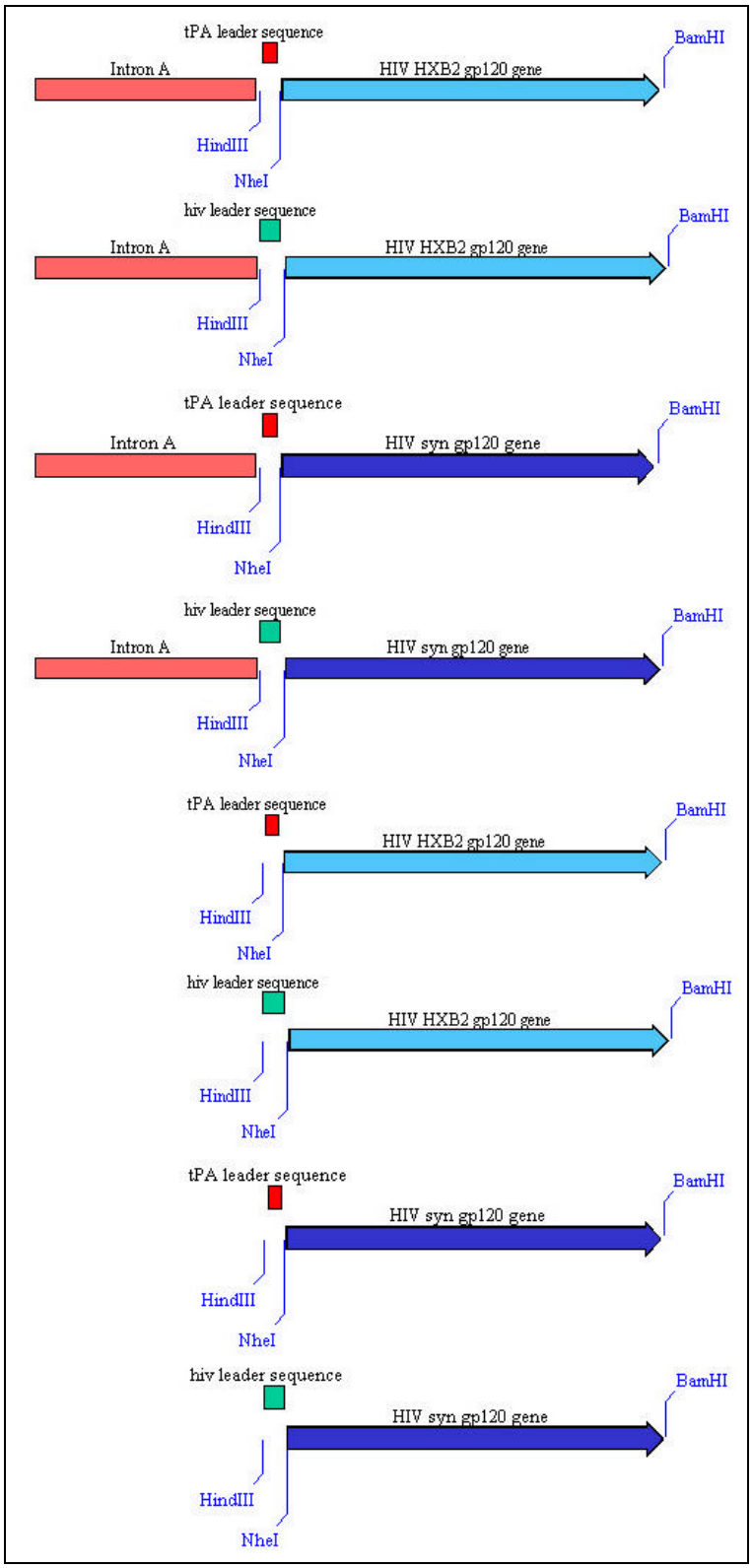

Figure 3a: eight constructs were used in the mouse experiment: with or without intron A, with tPA leader or HIV leader, and with codon optimization (syn) or without codon optimization (HXB2).

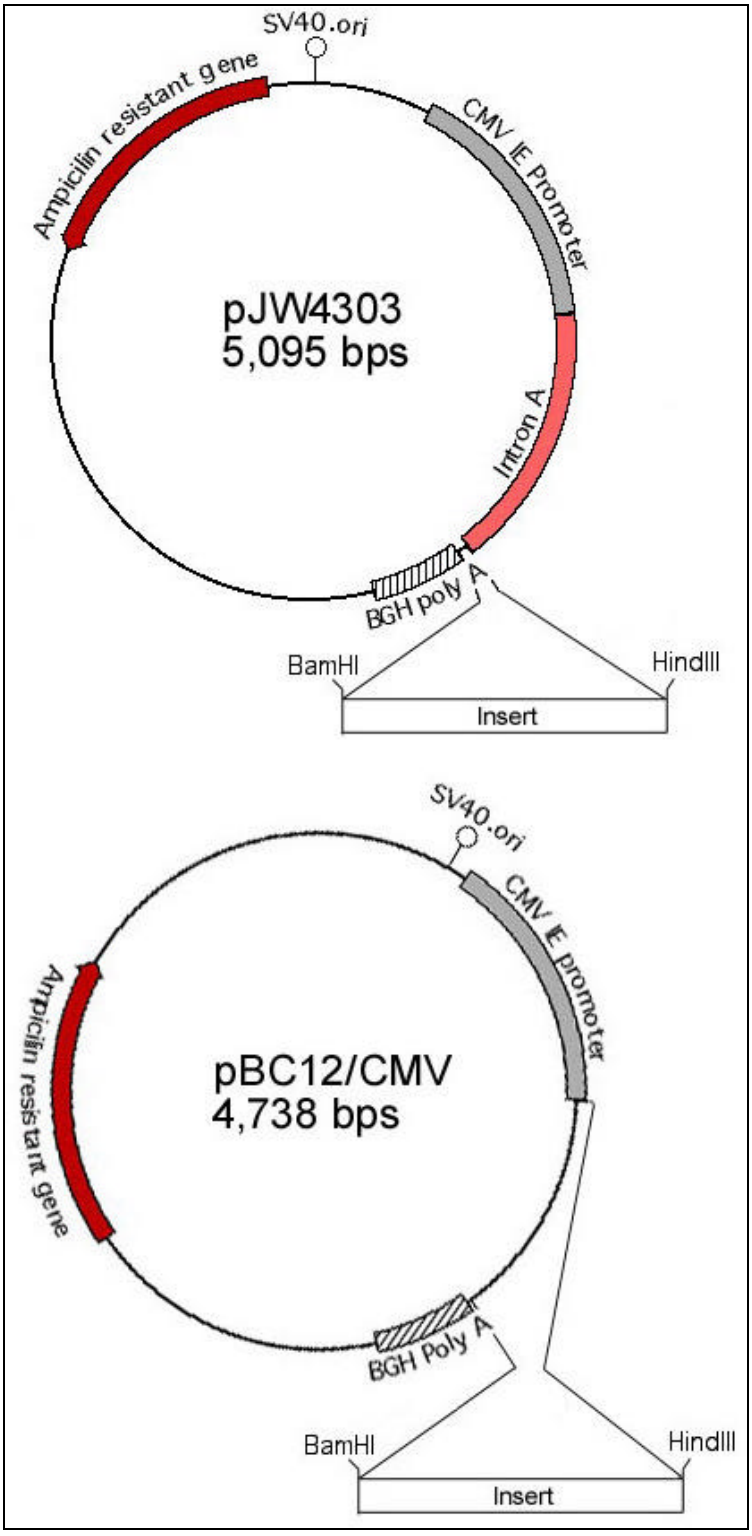

Figure 3b: Vectors used in the construction of the mouse experiment vaccine constructs. CMV IE gene Intron A is provided only by pJW4303.

RESULTS

Mouse Experiment: Antigen Optimization. Effects of Codon Optimization, tPA leader and Intron A

In this experiment the objective is to compare the immune response obtained from constructs differing in three variables: codon bias, leader or signal sequence, and spliceability. The effect of these variables on '*in vitro*' and '*in vivo*' expression has been tested in the past (Huang and Gorman, 1990; Chapman *et al.*, 1991; Cheng *et al.*, 1993; Luo and Reed, 1999; Kotsopoulou *et al.*, 2000; Xu *et al.*, 2001). Here, an immunological approach is provided, in which the importance of each of these elements is evaluated by measuring the immunogenicity of the different DNA vaccine constructs.

Two gp120s were tested, one codon-optimized, based on the amino acid sequence of the JR-FL strain. The other is a non-codon-optimized strain, HXB2. Both are members of the B clade, nevertheless, the optimal situation would have been to have a codon-optimized gp120 construct derived from the same strain as the non-codon optimized construct. This would allow for a stronger comparison, but this was not possible due to availability reasons. To circumvent this problem, both HXB2 and JR-FL (synthetic, syn) sera were tested against the homologous and heterologous antigens.

A codon usage comparison was made to proof that the codon usage of the codon-optimized construct was indeed closer to human genes, and that the codon usage of both HXB2 and non-optimized JR-FL HIV clones was similar. As seen in table IX, in 76 % of

the cases (16 out of 21 possible cases) codon usage for a given amino acid showed a clear pattern: HIV and JR-FL clustered together and syn and human clustered together in a different group.

Table IX: Codon usage comparison. Two HIV codon usage patterns (HXB2 & JR-FL), the codon-optimized codon usage pattern (syn), and the human Factor VII gene usage pattern (human) are compared. A percentage of the number of times a particular gene uses a determinate codon to code for a given amino acid is shown. The highest percentage for every gene and for every aminoacid is shaded.

			HIV		Human	
			HXB2	JR-FL	syn	Human
Codon		AA	Percent	Percent	Percent	Percent
TT	T	F	2.5	1.7	0.7	0.2
TT	C	F	1.3	1.2	2.4	2.3
TT	A	L	1.9	2.2	0	0.4
TT	G	L	0.8	1.9	0.2	0.6
TC	T	S	0.6	0.8	1.4	0.5
TC	C	S	0.6	0.4	0.7	2.2
TC	A	S	1.7	1.2	0.2	1.5
TC	G	S	0	0.2	0	0.1
TA	T	Y	2.1	1.9	0.7	0.7
TA	C	Y	0.2	0.8	1.5	1.2
TA	A	*	0	0.1	0	0.1
TA	G	*	0	0	0.2	0.6
TG	T	C	3.2	1.9	1.2	1.6
TG	C	C	0.6	0.7	2.4	3.7
TG	A	*	0	0	0	0.4
TG	G	W	2.1	3.2	1.9	2.2
CT	T	L	0.4	0.8	0.5	0.7
CT	C	L	0.4	1.7	0.5	2
CT	A	L	1.1	1.5	0.5	0.1
CT	G	L	1.1	1.8	6.2	4.6
CC	T	P	0.4	0.6	2.1	1.1
CC	C	P	1.3	0.9	3.3	2.2
CC	A	P	2.5	1.7	0.5	1.6
CC	G	P	0.2	0.2	0.3	0.5
CA	T	H	1.3	0.8	0.3	0.4
CA	C	H	0.2	0.5	1.5	5.4
CA	A	Q	2.1	2.1	0.3	1.2
CA	G	Q	1.7	2.5	3.4	4
CG	T	R	0.2	0.1	0.2	0.1
CG	C	R	0	0.2	0.3	1.3
CG	A	R	0	0.1	0	0.5
CG	G	R	0	0.1	0.2	1.7

Table IX (continued)

Codon		AA	HIV HXB2 Percent	HIV JR-FL Percent	Human syn Percent	Human Human Percent
AT	T	I	2.5	2.6	1.7	1
AT	C	I	1.7	1.2	4.6	2.2
AT	A	I	3.4	3.9	0.2	0.5
AT	G	M	1.9	1.9	2.1	2.1
AC	T	T	2.1	1.9	2.1	0.7
AC	C	T	1.9	1.8	5.3	1.5
AC	A	T	4.4	2.8	0.3	3.2
AC	G	T	0.6	0.6	0	1.7
AA	T	N	6.5	5.3	2.2	0.7
AA	C	N	2.3	1.7	5.3	1.5
AA	A	K	4.4	3.4	0.2	0.9
AA	G	K	2.1	1.5	5.2	2.1
AG	T	S	3	1.8	0.2	0.5
AG	C	S	1.9	1.2	3.4	1.7
AG	A	R	3.8	4	0.2	3.3
AG	G	R	0.4	1.5	4.3	1.2
GT	T	V	0.6	0.7	0	0.4
GT	C	V	1.1	1.1	0.7	2
GT	A	V	4.4	3.4	0.2	0.4
GT	G	V	1.1	1.7	6.4	2.6
GC	T	A	0.6	1.8	1.4	1
GC	C	A	1.1	1.1	3.4	2.2
GC	A	A	2.3	2.2	0.3	2
GC	G	A	0.2	0.4	0	1.1
GA	T	D	2.5	2	1.2	1.8
GA	C	D	1.5	1.5	2.6	2.8
GA	A	E	3.2	4.8	0	1.1
GA	G	E	1.7	1.7	6.2	4.3
GG	T	G	0.8	0.8	1.7	0.2
GG	C	G	0.2	0.7	3.3	3.7
GG	A	G	3.6	3.7	0	1.6
GG	G	G	1.5	1.7	1.7	2.6

'In vitro' Expression

In vitro expression was assayed. Western blots were run to compare the in vitro expression of the different constructs, and how the encoded protein was distributed in the intracellular and secreted fractions. This kind of comparison will give a first insight into the effect of the leader sequence on secretion, which is a determinant factor in the efficacy of the vaccine to raise a humoral immune response. The in vitro expression analysis will also reveal whether codon optimization and the presence of intron A actually contributed to increasing the overall expression levels. As seen in figure 4, the constructs with codon optimization had a higher overall expression as compared to the non codon-optimized constructs (HXB2). It is also remarkable that the expression falls dramatically in the non codon-optimized (HXB2) constructs when tPA and/or intron A are not present. To draw any conclusions from the distribution of the protein in supernatant and lysates, it is necessary to note that the lysate fraction is more concentrated than the supernatant, and that there is not an easy method to equalize the gp120 amount loaded from each fraction. For this reason, the comparisons should be made between the same fraction for two different constructs, e.g. compare the amount of protein present in the lysate of the codon-optimized construct with tPA with the amount of protein in the lysate of the codon-optimized construct without tPA. Following this rule, it is noticeable that secretion is augmented when tPA leader is included, especially when we look at the codon-optimized (syn) constructs. The band corresponding to the supernatants of the synthetic constructs with tPA (lane 5 panel A, and lane 5 panel B) is thicker than the same band for the constructs without tPA (lane 9 panel A, and lane 9 panel B). And the opposite effect is seen for the lysates (lane 6 panel A, and lane 6 panel

B, compared to lane 10 panel A, and lane 10 panel B). It is also noticeable that the lysates of the constructs without tPA leader (lane 10 panel A, lane 10 panel B) appear as a blurred band, probably due to misfolding or truncation of the nascent protein.

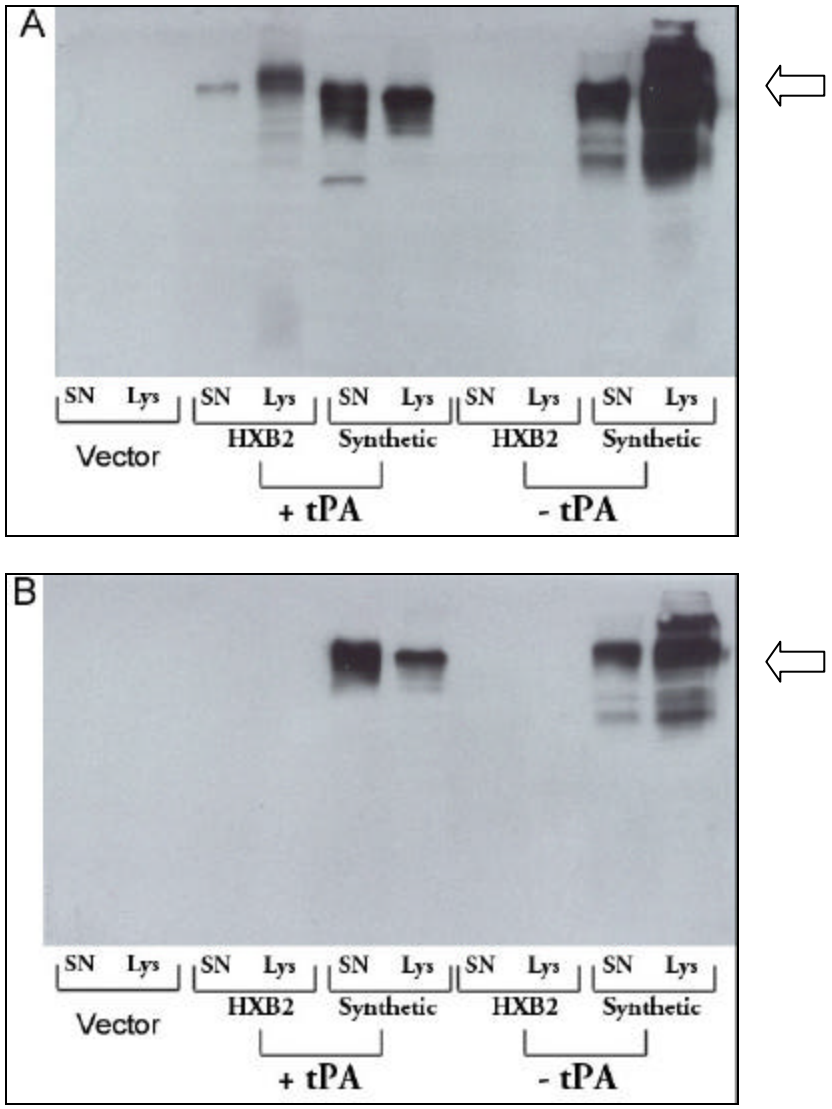

Figure 4: *'In vitro'* expression of the mouse experiment constructs. 293T cells were transfected with the different DNA vaccine constructs. Cell supernatants and lysates were collected and analyzed by western blot. Panel A corresponds to the constructs with intron A (pJW4303 vector), and panel B corresponds to the constructs without intron A (pBC12/CMV vector). The arrows indicate the position of gp120, although it can vary due to differences in glycosylation.

ELISA

As a measure of the specific antibody response mounted by the mice after being inoculated with the DNA vaccines, ELISAs were performed to quantitate the levels of anti-gp120 antibodies. Since the antigens encoded were slightly divergent in sequence, homologous and heterologous reactivity was measured. Each serum was tested against the same antigen used to immunize the mouse from which the serum was collected (homologous reactivity), and against the other antigen used in the experiment (heterologous reactivity). The results are shown in figure 5.

Overall, the codon optimized JR-FL (syn) construct had the highest reactivity. In the upper left panel (figure 5) it is shown how the reactivity decreased only slightly when intron A was not present, and a little more when the construct had the HIV leader sequence (tPA-) instead of the tPA leader sequence (tPA+). The effect of intron A was practically inconspicuous for the synthetic constructs, since the four curves clustered in two groups, two with tPA leader and two with HIV leader. In the upper right panel, the homologous reactivity for the HXB2 (non codon-optimized) constructs is shown. In this case, the presence of the tPA leader sequence also had an effect, only this time it was more dramatic. Intron A was required for the HXB2 constructs to show reactivity; even the construct with tPA leader but without intron A showed no reactivity.

As seen in the lower panels, heterologous reactivity was lower, consistent with the slight sequence divergence, although the pattern showed no major change. The exception was the reactivity of the antiserum from the mice immunized with the non-codon optimized (HXB2) gp120 with tPA and without Intron A construct, against the codon-optimized (syn) antigen (see figure 5, lower left panel). In this case the heterologous reactivity was higher than the homologous reactivity (see figure 5 upper right panel).

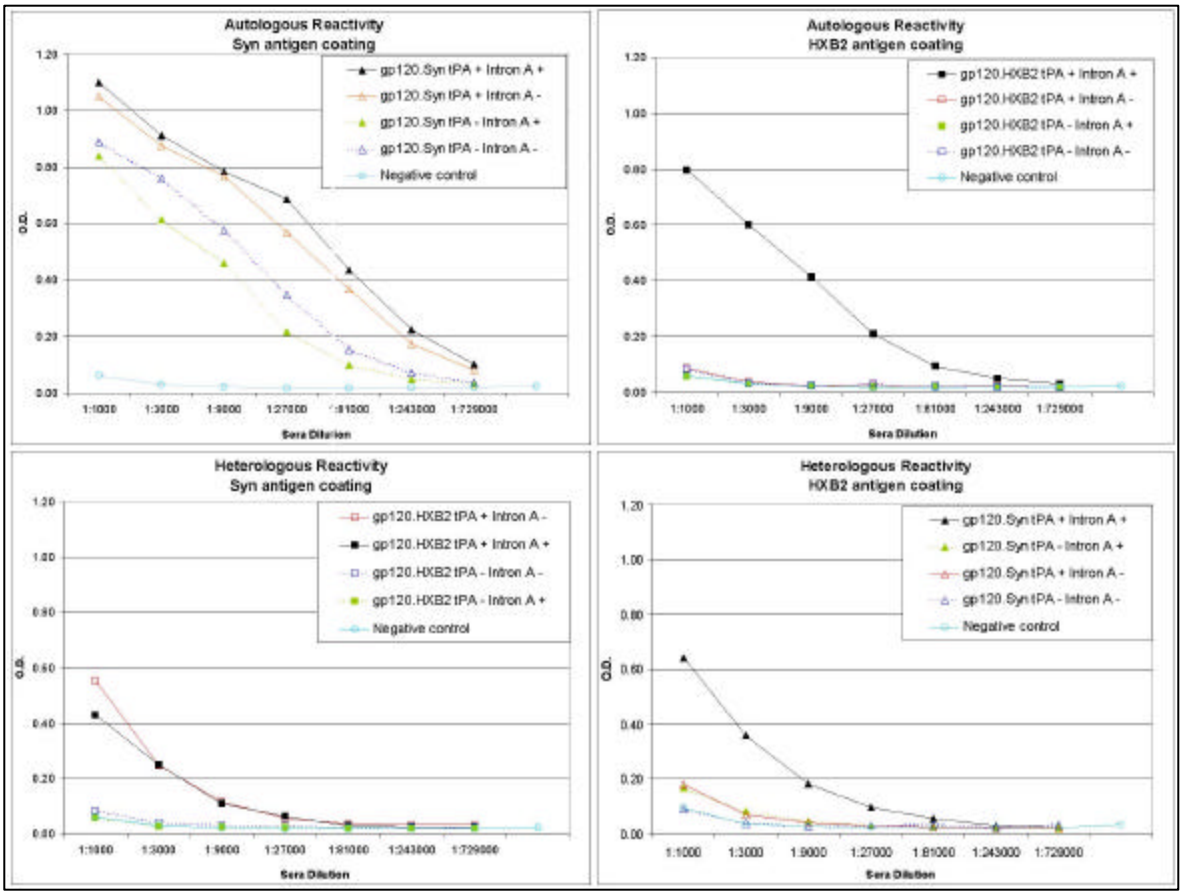

Figure 5: ELISA data for the mouse experiment. Antigens were produced from the DNA vaccine constructs by transfecting 293T cells. Each antigen, gp120.syn or gp120.HXB2 was used to coat two plates. The upper panels show the homologous sera reactivity, and the lower panels show the heterologous sera reactivity. OD at 450 nm was used as a measure of specific reactivity.

The time course of the humoral response was analyzed by ELISA. Only the groups that showed highest reactivity for each gp120 in the previous assay were analyzed (see figure 5). As it is shown in figure 6, the specific reactivity and the antibody titers were higher for the optimized JR-FL (syn) gp 120 constructs with intron A and with tPA leader than for the synthetic gp 120 with intron A but without tPA leader. Although at different levels, the response for both constructs followed the same pattern along time. Both the specific reactivity and the titer started showing from week 4 (after the first immunization), grew rapidly up to week 10 (after the third and last immunization), and remained stable up to week 12. Therefore, the humoral immune response observed was sustained for the animals immunized with these constructs. For the two HXB2 (non-codon optimized) constructs, the initial response was stronger (week 4, after first immunization), but it decreased with time. For the construct without Intron A, the response was not sustained and it decreased after the second immunization (week 8).

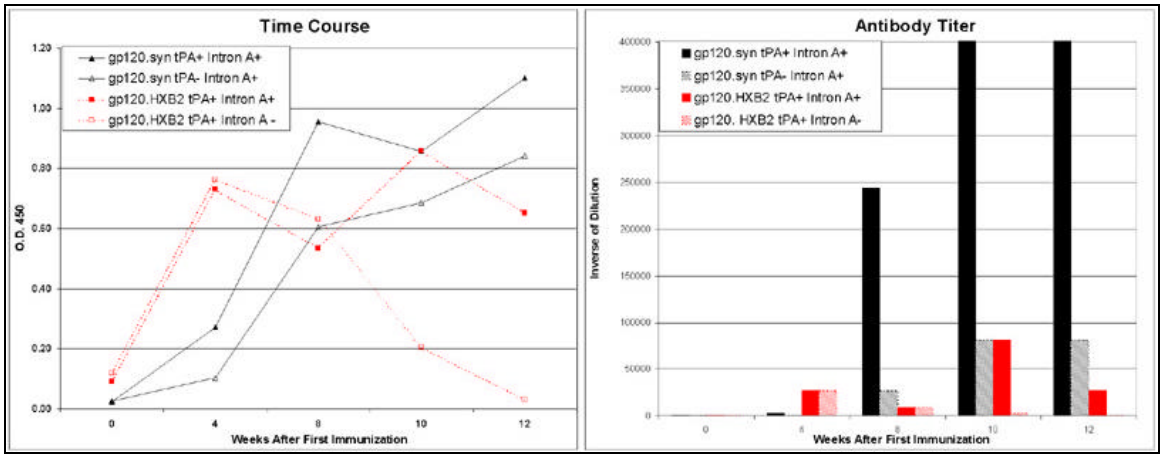

Figure 6: Time course of antibody reactivity and titer for the mouse experiment during 12 weeks after the first imunization. The left panel shows the ELISA reactivity against time. The right panel shows the antibody titers against time. The titer is measured as the inverse of the dilution indicated on the axis.

The subsequent figures (7, 8, and 9) were generated from the same set of data as figure 5. The data are rearranged to emphasize the effect of the three individual modifications: intron A (figure 7), codon optimization (figure 8) and tPA leader (figure 9).

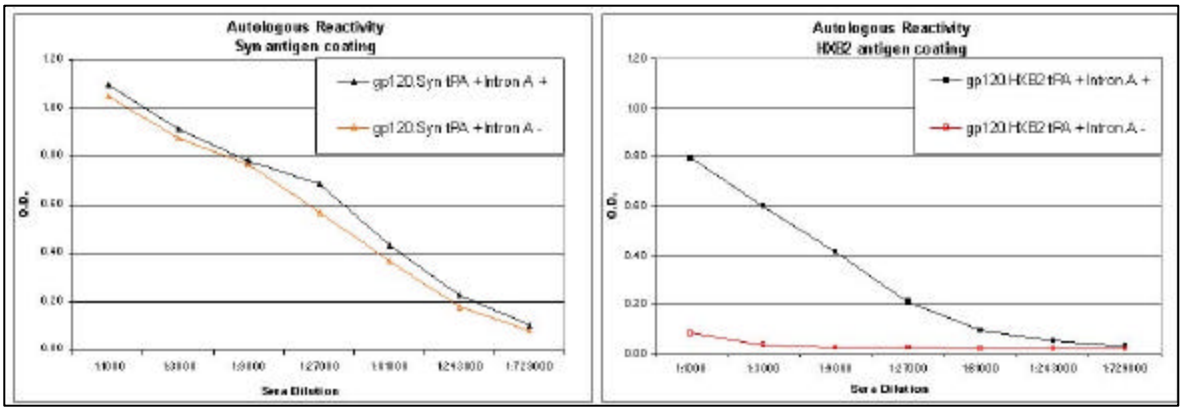

Figure 7: Role of encoded intron A in the antibody response obtained. The left panel shows specific antibody reactivity against codon-optimized constructs (syn) with or without intron A. The right panel shows specific antibody reactivity against non codon-optimized constructs (HXB2) with or without intron A.

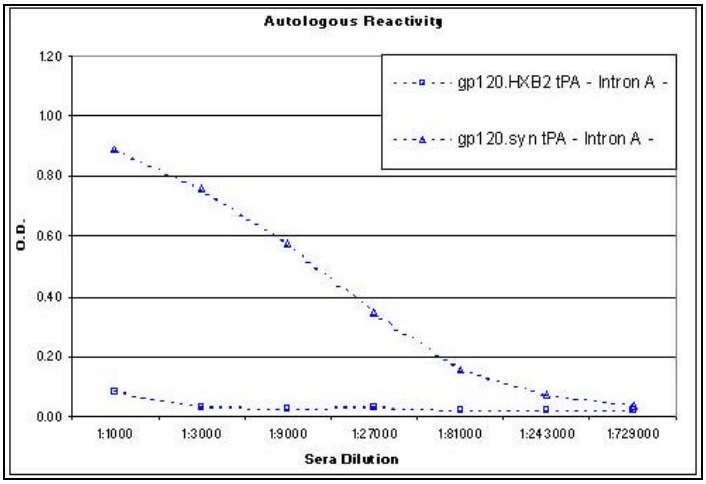

Figure 8: Effect of codon optimization. Autologous reactivity of sera from animals immunized with constructs without tPA and intron A, and with or without codon optimization.

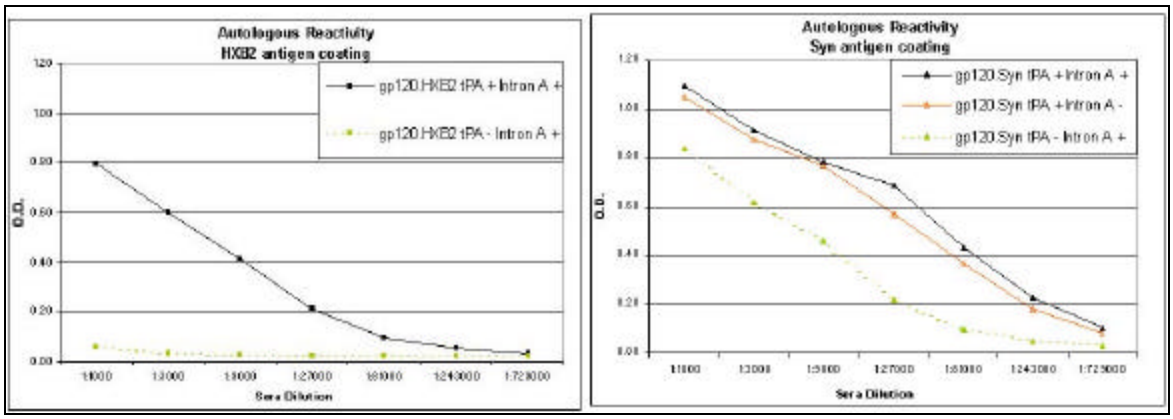

Figure 9: Effects of tPA leader sequence on the antibody response. The left panel shows specific antibody reactivity for sera from animals immunized with constructs encoding HXB2 (non codon-optimized) gp120 with intron A, and with or without the tPA leader sequence. On the right panel the same effect is shown for sera from animals immunized with codon-optimized constructs with or without tPA, and regardless of the presence of intron A.

ELISPOT

Mice were terminated and splenocytes were collected after the third immunization and after boosting with DNA one week prior to termination. They were stimulated in vitro with different peptides. The B peptides are based on the B clade and were expected to be cognate to the synthetic constructs, since these constructs were derived from the JR-FL strain, a clade B member. The HXB2 peptides are derived from the HXB2 IIIB strain of HIV-1, also a clade B member, and have been proven to be T-epitopes for gp120 HXB2 (Takeshita, *et al.*, 1995). The results in table X indicate a high IFN-γ production from the splenocytes of the mice immunized with the HXB2 (non-codon-optimized) construct with tPA leader and Intron A, after stimulation with the HXB2 IIIB peptides. The rest of the constructs show very low ? probably background ? reactivity. The ELISPOT assays were thus inconclusive, since the clade B peptides were not able to stimulate splenocytes from the mice immunized with the optimized JR-FL (denoted as 'syn') gp120 construct.

Table X: ELISPOT results. The splenocytes from the mice immunized with the different constructs were tested for specific IFN-g production after stimulation with homologous and heterologous peptides (see text above). Spots were counted per million cells.

Peptide: None Vaccine Construct		B V3 9-mer	B V3 15-mer	HXB2 IIIB 9-mer	HXB2 IIIB 15-mer
HXB2 Intron A+ tPA+	-	-	-	920	240
HXB2 Intron A+ tPA-	-	-	-	20	80
syn Intron A+ tPA+	-	-	-	60	80
syn Intron A+ tPA-	-	60	40	20	-
HXB2 Intron A- tPA+	-	40	40	40	-
HXB2 Intron A- tPA-	-	-	-	-	-
syn Intron A- tPA+	-	-	-	-	-
syn Intron A- tPA-	-	40	60	20	40
Con A Positive contro	1160	-	-	-	-

Rabbit Experiment: Epitope Exposure.
Molecular Cloning and Characterization of Deglycosylated gp 120 Vaccine Constructs

This experiment is to construct DNA vaccines in which the N-linked glycosylation sequence is mutated by substituting the Asparagine residue by a Glutamine, therefore removing the N-linked glycan at that particular site. Deglycosylation mutations were introduced by directed mutagenesis at particular sites in the tip of gp120's V1 loop, the area where glycosylation is suspected to be covering conserved epitopes. In figure 10 an alignment of the amino acid sequence covering the V1/V2 region of all the different clades is shown. The potential glycosylation sites in V1 are highlighted. Based on the structure of gp120 (figure 1), and on this alignment (figure 10), a pattern can be inferred for the glysosylation sites. There are N-linked glycosylation sites required for proper folding of the protein at either sides of the highly variable loop area. These N-linked glycosylation sites are located near cysteine residues involved in disulfide bond formation. These residues were left intact, since modifications in these residues will probably result in protein misfolding. The residues targeted in this thesis are located in the highly variable area of the V1 loop tip.

```
Clustal W(1.4) multiple sequence alignment

11 Sequences Aligned.         Alignment Score = 12363
Gaps Inserted = 23            Conserved Identities = 15

Pairwise Alignment Mode: Slow
Pairwise Alignment Parameters:
    Open Gap Penalty = 10.0   Extend Gap Penalty = 0.1
    Similarity Matrix: blosum

Multiple Alignment Parameters:
    Open Gap Penalty = 10.0   Extend Gap Penalty = 0.1
    Delay Divergent = 40%     Gap Distance = 8
    Similarity Matrix: blosum

Processing time: 0.6 seconds
                                V1 loop                                   V2 loop
                     ________________________________    ______________________________________________

gp120.A1   128                            CNATASNVTNEMRN C SFNITTELKDKKQQVYSLFYKLDVVQINE-K-----NETDKYRLINC 184
gp120.A2   128          CSYNITNNI------TNSITNSSVNMREEIKN C SFNMTTELRDKNRKVYSLFYKLDVVQINNGN-----NSSNLYRLINC 197
gp120.Bal  130        LNCTDLRNATNG--NDTNTTSSSREMMGGGEMKN C SFKITTNIRGKVQKEYALFYELDIVPIDN-------NSNNRYRLISC 203
gp120.B    128          CTNLRNDTNTTRNATNTTSS-ETMMEEGEIKN C SFNITTSIRDKVQKEFALFYKLDVVPIEN-------DTTS-YRLISC 199
gp120.C1   128          CSNRTIDYN-----------NRTDNMGGEIKN C SFNMTTEVRDKREKVHALFYRLDIVPLKNESS----NTSGDYRLINC 193
gp120.C2   128          CTNANGTNN-------NGTVNVNDTMYGEIKN C SFNMTTELRDKKKQVYALFYKLDIVSLNENS-----NNSSEYRLINC 196
gp120.CZM  128          CTEVNVTRNVN-NSVVNNTTNVNNSMNGDMKN C SFNITTELKDKKKNVYALFYKLDIVSLNETDDSETGNSSKYYRLINC 207
gp120.D    128          CTEWKNATTN------------ATNEGIGMKN C SF---TEVRDKKKQAYALFYKLDVVQMNDDN-----STNTSYRLINC 188
gp120.E    135CTNATLNCTNLTNGNK------TTNVSNIIGNLTDEVRN C SFHMTTELRDKKQKVYALFYKLDIVQIN----------SSEYRLINC 206
gp120.F    128          CRNIATNGTN----DTIATNDSLKEDPWAIQN C SFNTTTEIRDKQLKVHALFYKLDIVLINQ-------NDNRTYRLIHC 197
gp120.G    128          CANVTNNYT--------ELANTSIGNREEIKN C SFKVTTELRNKQKEEYALFYRTDVIPINDNSKS-SASNYSDYRLINC 199

Consensus               CTN . . N                   EIKN C SFN.TTELRDK..KVYALFYKLDIV INN            YRLINC
```

Figure 10: Clustal W alignment of the V1/V2 regions of gp120 in different HIV-1 clades. The dashes represent gaps. Asterisks represent highest homology, and dots represent a lower degree of homology. The parameters of the alignment are shown on top. The highly variable regions correspond to the tips of the V1 and V2 loops. The Asn residues susceptible to N-linked glycosylation in the V1 loop are highlighted.

Molecular Cloning

In figure 11 a map is shown of the deglycosylated gp120 clade G vaccine construct. Two segments are cloned into the Pst I – Bam HI fragment of the vector. Each of the segments is a digested PCR product from each of the two PCR reactions conducted to generate the mutations. The Sac I site in between the two segments was introduced with the PCR primers to facilitate screening.

.

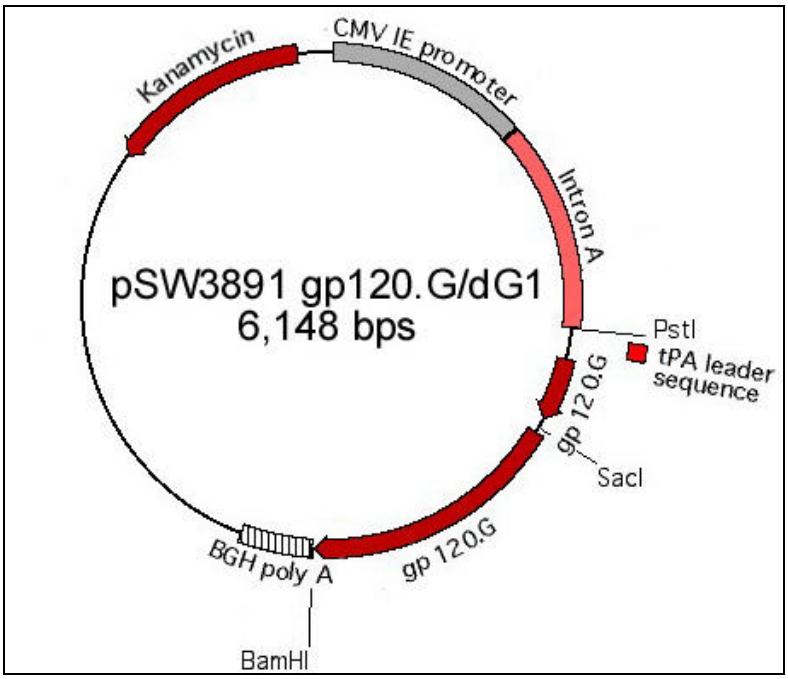

Figure 11: map of one of the deglycosylated constructs obtained, the deglycosylated gp120 clade G. Note the presence of the newly introduced Sac I site.

The transformants were screened by restriction digestion, and in the selected clones the sizes obtained after analytic digestions coincided with the expected sizes, as shown in figure 12.

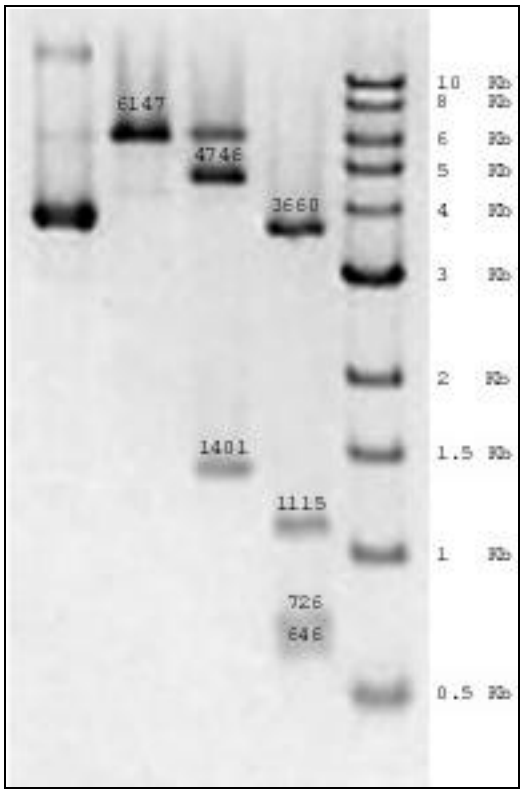

Enzyme Used for Digestion	Expected Fragment Size(s)		
	Bam HI	Bam HI + Nhe I	Sac I
	6147	4746 1401	3660 1115 726 646

Figure 12: Analytic digestions were performed for the deglycosylated gp120.G clone (pSW3891/gp120.GdG1) to check for the correct sizes before testing expression. Lane 1: uncut plasmid. Lane 2: Bam HI, Lane3: Bam HI + Nhe I, Lane 4: Sac I, Lane 5: 1 Kb ladder. Fragment size predictions are shown on the chart on the right.

'In vitro' Expression

Expression of all the constructs was assessed by western blot. DNAs from wild-type and deglycosylated constructs were transfected in parallel, cell supernatants and lysates were collected, and an SDS-PAGE and a western blot were run. All constructs expressed well (figure 13) and a band shift was observed when comparing each wild-type band with its deglycosylated counterpart (figures 13 and 14).

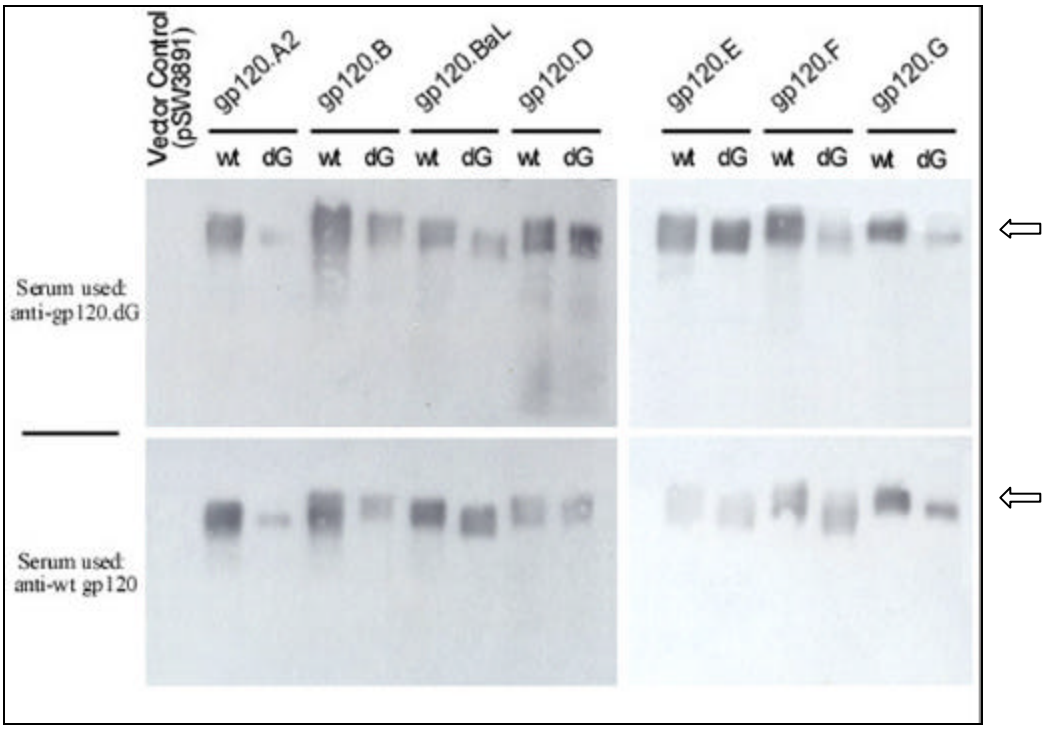

Figure 13: Western blot comparing the expression of wild-type and the deglycosylated constructs. The upper panels used a serum from animals immunized with a polyvalent vaccine combining all the wild-type DNA vaccine constructs. In the lower panels, the serum used was raised against a polyvalent vaccine combining all the deglycosylated DNA vaccine constructs. pSW3891 vector was used as a negative control. The arrows point at the position of gp120.

As seen in figure 13, deglycosylated antigens were recognized by wild-type-raised sera and vice-versa. Thus, the deglycosylated protein did not lose its conformation, since it can be recognized by a serum raised against wild-type gp120. Also, the band shift observed in more detail in figure 14, shows that the deglycosylations encoded in the vaccines actually occurred '*in vitro*'.

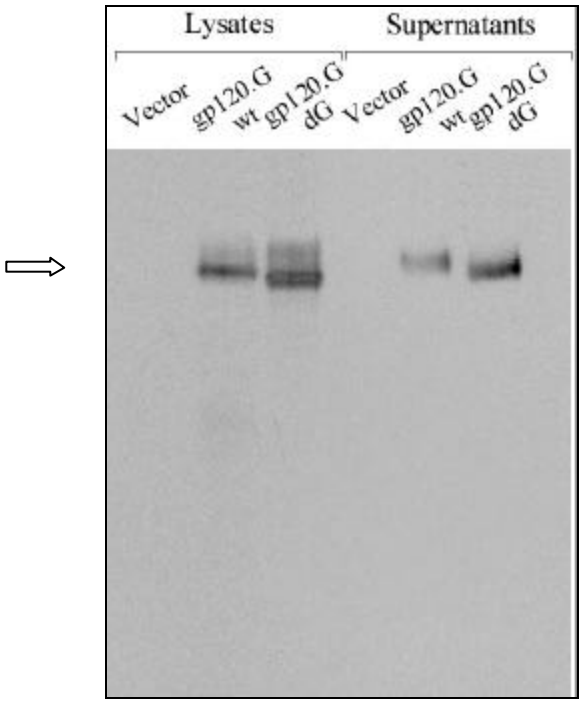

Figure 14: Western blot comparing the electrophoretic mobility of the wild-type and the deglycosylated gp120 clade G. The serum used was raised from rabbits immunized with wild-type gp120 clade G. pSW3891 vector was used as a negative control. The arrow shows the position of gp120.

Following acquisition of these data, the deglycosylated vaccine constructs cloning and characterization was concluded. Rabbit immunizations were also performed, and the sera were collected for further analysis, e.g. ELISA and neutralization assays, but these experiments will not be detailed in this thesis.

DISCUSSION

Antigen Optimization: Effects of Codon Optimization, tPA Leader and Intron A

Four steps must occur for gp120 protein secretion: first mRNA is synthesized from proviral DNA, then it is transported to the cytoplasm, and translation starts. The signal peptide targets the nascent protein to the endoplasmic reticulum, where synthesis is resumed. Finally, the protein goes through the Golgi to the extracellular space.

The first step influenced by our modifications is the transport of mRNA to the cytoplasm. Both the codon-optimized and the non-optimized HXB2 constructs are Rev-independent, since they lack the Rev response element (RRE). Rev is also responsible for stabilization of instability sequences (INS) present in HIV gag-pol mRNAs (Schwartz *et al.*, 1992). Nevertheless, codon optimized constructs have a completely different nucleotide sequence, so no INS are present. This should result in cytoplasmic mRNA levels higher than those for the HXB2 mRNA. The mRNA levels have not been tested, but this assumption is made based on previous studies regarding the role of INS in gag-pol mRNA levels (Schwartz *et al.*, 1992; Schneider *et al.*, 1997). However, the existence of instability sequences in the env mRNA has only been demonstrated in the region overlapping the Rev Responsive Element (RRE) (Brighty *et al.*, 1994). In our case, the RRE is not included in the cloned fragment of env, so if there was any effect of codon optimization on mRNA transport or instability it would be dependent on putative sequences homologous to the ones found in gag-pol, but whose presence has not yet been

proven. From the results, it is clear that the antibody response was always higher for the codon-optimized constructs (figure 5), which reflects higher '*in vivo*' expression levels from the DNA vaccine. This might be due to the better tRNA availability, the putative positive effect of codon optimization on mRNA transport and stabilization, or both.

The presence of intron A in the pre-mRNA also influences this nuclear export step. It is known that a spliceable transcript is more stable and yields higher cytoplasmic mRNA levels in mammalian expression systems (Luo *et al.*, 1999). Transcription factor binding site homology sequences have been detected inside the sequence of intron A. This would have an effect in transcription form the CMV IE promoter. Several studies have been conducted to investigate the effects of introns in the expression levels obtained from plasmid vectors (Chapman *et al.*, 1991; Cheng *et al.*, 1993; Xu *et al.*, 2001). Intron A is the largest of the four introns in the Cytomegalovirus immediate early gene. The promoter/enhancer region of this gene has proven one of the most powerful in mammalian expression vectors (Cheng *et al.*, 1993). Two mechanisms have been proposed as responsible for the increased expression levels provided by the presence of intron A: mRNA stabilization and transport to cytoplasm (Huang *et al.*, 1990; Luo *et al.*, 1999), and binding of transcription factors (Chapman *et al.*, 1991). In that study, a consensus-binding site for transcriptional activator NF1 was found in the intron A sequence. Mutations in that sequence triggered a decrease in the expression levels of reporter genes '*in vitro*'. Retardation gel experiments showed how the mutated sequences were less efficient in binding NF1, although this difference could not account for the expression differences observed when comparing constructs with or without intron A,

leaving other factors such as nuclear export as a possible explanation for this effect. The augmented expression observed in that study when intron A was included was not as evident when transcription occurred from SV40 early promoter instead of CMV IE promoter. Because of these reasons it is expected that those constructs carry intron A will show an increase in the expression levels. Data presented in this thesis did show an increase in ELISA signal for gp120 from mice sera when comparing codon optimized constructs with or without Intron A, although it was not a dramatic increase (see figure 7). If we speculate with the possibility of the presence of instability sequences on env, intron A should not affect cytoplasmic mRNA levels of codon-optimized constructs as much as it does for the HXB2 (non-codon optimized) constructs. Since the cytoplasmic mRNA levels of the codon-optimized constructs are presumed to be already high due to the lack of instability sequences, an additional enhancement from intron A would not as conspicuous as it is for the HXB2 constructs. This effect is shown in figure 7: for the non-codon optimized constructs the antibody production was markedly different when comparing constructs with or without intron A, whereas the difference is very small when the codon-optimized constructs with and without intron A are compared.

A codon bias closer to mammalian codon bias will expectedly enhance protein synthesis from viral mRNA. In our case, this would happen when the construct is codon optimized, as reflected by the higher specific antibody reactivity shown in figure 5. tRNA availability is more favorable to the constructs with a mammalian codon bias. From my results, this translation step cannot be discerned from the nuclear export, since mRNA was not measured. Nevertheless, the antibody production in constructs differing only in

codon optimization and without any of the other elements is markedly different, as seen in figure 8.

Secretion is at the end of the protein synthesis pathway. The effect of enhanced secretion is appreciable only when the levels of intracellular protein are high, i.e. when the constructs carry either codon optimization or intron A, or both. The incorporation of a tPA leader should yield higher protein levels in the extracellular space. As seen in other studies (Chapman *et al.*, 1991), the substitution of HIV leader sequence by the tPA leader sequence led to a substantial increase in expression levels of env protein. In the constructs featured in figure 9, protein synthesis was enhanced either by codon optimization or by the presence of intron A; therefore the effect of tPA leader inclusion is evident.

The mechanism underlying the inefficiency of HIV leader has been proposed (Li *et al.*, 1994, 2000; Martoglio *et al.*, 1997). According to these studies, the env signal sequence has particular characteristics distant from the expected for a typical signal sequence, which retards its own cleavage. The protein cannot start folding until cleavage of the signal sequence has occurred. The HIV signal sequence contains 5 positively charged amino acids in the N-terminal region, which is very uncommon for a signal sequence (see table VIII). It was observed that the presence of these residues did not influence the translocation into the endoplasmic reticulum (ER), but the cleavage of the signal sequence and therefore the protein folding (Li *et al.*, 1994; Pancino *et al.*, 1994). Experiments measuring gp140 and gp120 association with calnexin – an ER protein that

binds protein precursors while they still contain the signal sequence – showed a slow signal sequence cleavage kinetics. The correlation of this slow kinetics with folding was established by measuring disulfide bond formation and the precursor's ability to interact with CD4. Uncleaved protein remains in the ER, leading to aggregation and misfolding. In figure 9, the lyates from the cells transfected with the constructs without tPA appeared as a smeared band spanning a long size range. This observation is consistent with the high likelihood of proteins with HIV leader to misfold or to aggregate. More sound proof of the HIV leader retarding protein folding and secretion was obtained by the construction of a chimeric VSV-G protein containing the HIV leader sequence (Li *et al.*, 2000). A putative immune system evasion role has been proposed for HIV signal sequence by which a retardation of the protein folding would lead to a decreased MHC-I antigen presentation (Srinivas *et al.*, 1993; Martoglio *et al.*, 1997). My antibody production results are definitely consistent with these previous studies, showing an effect on protein expression rate dependent on the leader sequence. Nevertheless, the high antibody levels observed from the animals immunized with the codon-optimized construct with the HIV leader sequence are more difficult to explain. It is possible that a better tRNA availability drove the protein synthesis forward once the leader sequence is already inside the endoplasmic reticulum, although whether this is enough to balance the impaired cleavage ability of HIV leader remains unknown.

When comparing the reactivity of the antiserum from the mice immunized with HXB2 gp120 with tPA and without Intron A construct (gp120.HXB2 tPA+ Intron A-), against the codon-optimized (syn) antigen (see figure 5, lower left panel) and against the

HXB2 antigen (see figure 5 upper right panel), an interesting effect was seen: the heterologous reactivity was higher than the homologous reactivity. There is a possible explanation for this effect, and it is that the conformation of HXB2 gp120 *'in vivo'* was slightly different than *'in vitro'* whereas the conformation of the synthetic gp120 was closer *'in vitro'* and *'in vivo'*. Assuming that both gp120s shared an epitope that was present '*in vivo*', and that this epitope disappeared '*in vitro*' only in the HXB2 gp120, antibodies would be raised against that particular epitope *'in vivo'*. When reactivity was tested against the HXB2 antigen produced '*in vitro*', this epitope was not present and these antibodies were not reactive. When the heterologous reactivity was tested, the antigen was the synthetic gp120, which conserved the mentioned epitope *'in vitro'*, therefore the sera was reactive against this epitope and this accounted for the higher heterologous reactivity.

Unfortunately, the cell mediated immunity assays were not successful. The HXB2 III B peptides had been used before and the results obtained here replicated the ones obtained before (personal communication from Dr. Wang). This peptide has been proven to be a T-cell epitope (Takeshita *et al.*, 1995). Nevertheless, the B V3 peptides had not been tested before against a JR-FL construct (the codon optimized, syn constructs). It was assumed that they might react as well with JR-FL gp120, since both JR-FL and B gp120s are clade B. Without a positive reaction against the peptides that were supposed to be homologous for JR-FL, it is impossible to make a comparison between the different constructs, as it was done for the antibody response analysis. Therefore, the results from the cell-mediated immunity assays are inconclusive.

Epitope Exposure:
Molecular Cloning and Characterization of Deglycosylated gp120 Vaccine Constructs

This far, the deglycosylated constructs have been cloned and characterized, and the vaccinations have been performed. All the clones were expressed '*in vitro*'. From the western blot analysis, it can be concluded that the deglycosylated protein did not lose its conformation, since it can be recognized by a serum raised against wild-type gp120. Nevertheless, this is not enough evidence to prove the postulated epitope exposure upon deglycosylation. Future experiments could provide evidence supporting the postulated epitope exposure. This will require performing specific antibody reactivity assays and neutralization assays, which will not be covered in this thesis. The ELISAs have already been started, and the neutralization assays will be soon performed by Dr. Moubdjeka from the Nucleic Acid Vaccine Laboratory.

PERSPECTIVES

The present thesis has shown a series of attempts to improve gp120 immunogenicity. Cloning and characterization of the optimized vaccine constructs has already been achieved. Also, preliminary evidence is supplied as to the expected efficacy of the modifications introduced. At this point more palpable proof needs to be provided, e.g. neutralization assay data. These experiments have all been conducted in mice and rabbits, it is necessary to advance in the evolutionary scale and reproduce them in primates before going into a clinical trial. Both the neutralization assays and the macaque studies will be very soon conducted by Dr. Lu's laboratory and by our private partner Advance Bioscience Laboratories.

Another layer can be added to the modifications already depicted. Myself and other lab members are conducting experiments to generate a vaccine construct encoding gp120 plus the primary receptor CD4 and the co-receptor CCR5 or CXCR4. These proteins are going to be encoded in trans, separately or as fusion proteins comprising the extracellular domains of the co-receptor, CD4 and gp120. It has been previously shown how the interaction of gp120 with CD4 triggers the appearance of hidden epitopes (Thali *et al.*, 1993; Carrillo and Ratner, 1996; Trkola *et al.*, 1996); and how the formation of the tripartite protein complex leads to the exposure of the fusogenic domain of gp120. This raises the possibility to produce stable complexes '*in vivo*' through DNA vaccination as a further attempt to raise neutralizing antibody.

Once we have successfully tested the codon optimized construct, codon optimization is being expanded to every gp120 subspecies constructs. At this point, we have cloned and tested the *'in vitro'* expression of several optimized gp120 constructs plus an optimized Gag construct.

As a refinement of the codon optimization experiment, a Fluorescence *In Situ* Hybridization (FISH) experiment is being conducting to compare the subcellular location of the vaccine RNAs generated by codon optimized constructs versus the non-optimized RNAs. It is expected to observe a difference in location and in nuclear transport efficiency. This experiment is being conducted in collaboration with Polly Xing, M.D., Ph.D.

BIBLIOGRAPHY

Binley J, Sanders R, Clas B, Schuelke N, Master A, Guo Y, Kajumo F, Anselma D, Maddon P, Olson W, Moore J (2000). A recombinant human immunodeficiency virus type 1 envelope glycoprotein complex stabilized by an intermolecular disulfide bond between the gp120 and gp41 subunits is an antigenic mimic of the trimeric virion associated structure. J Virol. Jan 74(2): 627-643

Bohm W, Kuhrober A, Paier T, Mertens T, Reimann J, Schirmbeck R (1996). DNA vector constructs that prime hepatitis B surface antigen-specific cytotoxic T lymphocyte and antibody responses in mice after intramuscular injection. J Immunol Methods. Jun 14;193(1):29-40.

Brighty DW, Rosenberg M (1994). A cis-acting repressive sequence that overlaps the Rev-responsive element of human immunodeficiency virus type 1 regulates nuclear retention of env mRNAs independently of known splice signals. Proc Natl Acad Sci U S A. Aug 30;91(18):8314-8.

Cao J, Sullivan N, Desjardin E, Parolin C, Robinson J, Wyatt R, Sodroski J. (1997). Replication and neutralization of human immunodeficiency virus type 1 lacking the V1 and V2 variable loops of the gp120 envelope glycoprotein. J Virol. Dec;71(12):9808-12.

Carrillo A, Ratner L. (1996). Cooperative effects of the human immunodeficiency virus type 1 envelope variable loops V1 and V3 in mediating infectivity for T cells.J Virol. Feb;70(2):1310-6.

Cella M, Sallusto F, Lanzavecchia A (1997). Origin, maturation and antigen presenting function of dendritic cells. Curr Opin Immunol. Feb;9(1):10-6. Review.

Chackerian B, Rudensey LM, Overbaugh J. (1997). Specific N-linked and O-linked glycosylation modifications in the envelope V1 domain of simian immunodeficiency virus variants that evolve in the host alter recognition by neutralizing antibodies. J Virol. Oct;71(10):7719-27.

Chapman BS, Thayer RM, Vincent KA, Haigwood NL (1991). Effect of intron A from human cytomegalovirus (Towne) immediate-early gene on heterologous expression in mammalian cells. Nucleic Acids Res. Jul 25;19(14):3979-86.

Cheng L, Ziegelhoffer PR, Yang NS (1993). In vivo promoter activity and transgene expression in mammalian somatic tissues evaluated by using particle bombardment. Proc Natl Acad Sci U S A. May 15;90(10):4455-9.

Chow YH, Huang WL, Chi WK, Chu YD, Tao MH (1997). Improvement of hepatitis B virus DNA vaccines by plasmids coexpressing hepatitis B surface antigen and interleukin-2. J Virol. Jan;71(1):169-78.

Doe B, Steimer KS, Walker CM (1994). Induction of HIV-1 envelope (gp120)-specific cytotoxic T lymphocyte responses in mice by recombinant CHO cell-derived gp120 is enhanced by enzymatic removal of N-linked glycans. Eur J Immunol. Oct;24(10):2369-76.

Dumonceaux J, Nisole S, Chanel C, Quivet L, Amara A, Baleux F, Briand P, Hazan U. (1998). Spontaneous mutations in the env gene of the human immunodeficiency virus type 1 NDK isolate are associated with a CD4-independent entry phenotype. J Virol. Jan;72(1):512-9.

Drummer HE, Jackson DC, Brown LE. (1993). Modulation of CD4+ T-cell recognition of influenza hemagglutinin by carbohydrate side chains located outside a T-cell determinant.Virology. Jan;192(1):282-9.

Edinger AL, Mankowski JL, Doranz BJ, Margulies BJ, Lee B, Rucker J, Sharron M, Hoffman TL, Berson JF, Zink MC, Hirsch VM, Clements JE, Doms RW. (1997). CD4-independent, CCR5-dependent infection of brain capillary endothelial cells by a neurovirulent simian immunodeficiency virus strain. Proc Natl Acad Sci U S A. Dec 23;94(26):14742-7.

Endres MJ, Clapham PR, Marsh M, Ahuja M, Turner JD, McKnight A, Thomas JF, Stoebenau-Haggarty B, Choe S, Vance PJ, Wells TN, Power CA, Sutterwala SS, Doms RW, Landau NR, Hoxie JA. (1996). CD4-independent infection by HIV-2 is mediated by fusin/CXCR4. Cell. Nov 15;87(4):745-56.

Etemad-Moghadam B, Sun Y, Nicholson EK, Fernandes M, Liou K, Gomila R, Lee J, Sodroski J. (2000). Envelope glycoprotein determinants of increased fusogenicity in a pathogenic simian-human immunodeficiency virus (SHIV-KB9) passaged in vivo. J Virol. May;74(9):4433-40.

Fenouillet E, Gluckman JC, Bahraoui E. (1990). Role of N-linked glycans of envelope glycoproteins in infectivity of human immunodeficiency virus type 1. J Virol. Jun;64(6):2841-8.

Fynan EF, Webster RG, Fuller DH, Haynes JR, Santoro JC, Robinson HL (1993). DNA vaccines: protective immunizations by parenteral, mucosal, and gene-gun inoculations. Proc Natl Acad Sci U S A. Dec 15;90(24):11478-82.

Gao F, Morrison SG, Robertson DL, Thornton CL, Craig S, Karlsson G, SodroskiJ, Morgado M, Galvao-Castro B, von Briesen H, et al. (1996). Molecular cloning and analysis of functional envelope genes from human immunodeficiency virus type 1 sequence subtypes A through G. The WHO and NIAID Networks for HIV Isolation and Characterization. J Virol. Mar;70(3):1651-67.

Gilkeson GS, Pippen AM, Pisetsky DS (1995). Induction of cross-reactive anti-dsDNA antibodies in preautoimmune NZB/NZW mice by immunization with bacterial DNA. J Clin Invest. Mar;95(3):1398-402.

Gregoriadis G, Saffie R, Hart SL (1996). High yield incorporation of plasmid DNA within liposomes: effect on DNA integrity and transfection efficiency. J Drug Target.;3(6):469-75.

Haas J, Park EC, Seed B (1996). Codon usage limitation in the expression of HIV-1 envelope glycoprotein. Curr Biol. Mar 1;6(3):315-24.

Hartikka J, Sawdey M, Cornefert-Jensen F, Margalith M, Barnhart K, Nolasco M, Vahlsing HL, Meek J, Marquet M, Hobart P, Norman J, Manthorpe M. (1996). An improved plasmid DNA expression vector for direct injection into skeletal muscle. Hum Gene Ther. Jun 20;7(10):1205-17.

Huang MT, Gorman CM (1990). Intervening sequences increase efficiency of RNA 3' processing and accumulation of cytoplasmic RNA. Nucleic Acids Res. Feb 25;18(4):937-47.

Hsu CH, Chua KY, Tao MH, Lai YL, Wu HD, Huang SK, Hsieh KH (1996). Immunoprophylaxis of allergen-induced immunoglobulin E synthesis and airway hyperresponsiveness in vivo by genetic immunization. Nat Med. May;2(5):540-4.

Iwasaki A, Torres CA, Ohashi PS, Robinson HL, Barber BH (1997). The dominant role of bone marrow-derived cells in CTL induction following plasmid DNA immunization at different sites. J Immunol. Jul 1;159(1):11-4.

Jackson DC, Drummer HE, Urge L, Otvos L Jr, Brown LE. (1994). Glycosylation of a synthetic peptide representing a T-cell determinant of influenza virus hemagglutinin results in loss of recognition by CD4+ T-cell clones. Virology. Mar;199(2):422-30.

Kim JJ, Ayyavoo V, Bagarazzi ML, Chattergoon MA, Dang K, Wang B, Boyer JD, Weiner DB (1997). In vivo engineering of a cellular immune response by coadministration of IL-12 expression vector with a DNA immunogen. J Immunol. Jan 15;158(2):816-26.

Kolchinsky P, Kiprilov E, Bartley P, Rubinstein R, Sodroski J. (2001). Loss of a single N-linked glycan allows CD4-independent human immunodeficiency virus type 1 infection by altering the position of the gp120 V1/V2 variable loops. J Virol. Apr;75(7):3435-43.

Kotsopoulou E, Kim VN, Kingsman AJ, Kingsman SM, Mitrophanous KA (2000). A Rev-independent human immunodeficiency virus type 1 (HIV-1)-based vector that exploits a codon-optimized HIV-1 gag-pol gene. J Virol. May;74(10):4839-52.

Krieg AM, Yi AK, Matson S, Waldschmidt TJ, Bishop GA, Teasdale R, Koretzky GA, Klinman DM (1995) CpG motifs in bacterial DNA trigger direct B-cell activation. Nature. Apr 6;374(6522):546-9.

Krieg AM, Love-Homan L, Yi AK, Harty JT (1998). CpG DNA induces sustained IL-12 expression in vivo and resistance to Listeria monocytogenes challenge. J Immunol. Sep 1;161(5):2428-34.

Kwong PD, Wyatt R, Robinson J, Sweet RW, Sodroski J, Hendrickson WA. (1998). Structure of an HIV gp120 envelope glycoprotein in complex with the CD4 receptor and a neutralizing human antibody. Nature. Jun 18;393(6686):648-59.

Kypr J, Mrazek J (1987). Unusual codon usage of HIV. Nature. May 7-13;327(6117):20.

Lee WR, Syu WJ, Du B, Matsuda M, Tan S, Wolf A, Essex M, Lee TH (1992). Nonrandom distribution of gp120 N-linked glycosylation sites important for infectivity of human immunodeficiency virus type 1. Proc Natl Acad Sci U S A. Mar 15;89(6):2213-7.

Li Y, Luo L, Thomas DY, Kang CY. (1994). Control of expression, glycosylation, and secretion of HIV-1 gp120 by homologous and heterologous signal sequences. Virology. Oct;204(1):266-78.

Li Y, Luo L, Thomas DY, Kang CY. (2000). The HIV-1 Env protein signal sequence retards its cleavage and down-regulates the glycoprotein folding. Virology. Jul 5;272(2):417-28.

Lu S, Wyatt R, Richmond JF, Mustafa F, Wang S, Weng J, Montefiori DC, Sodroski J, Robinson HL. (1998). Immunogenicity of DNA vaccines expressing human immunodeficiency virus type 1 envelope glycoprotein with and without deletions in the V1/2 and V3 regions. AIDS Res Hum Retroviruses. Jan 20;14(2):151-5.

Luo MJ, Reed R (1999). Splicing is required for rapid and efficient mRNA export in metazoans. Proc Natl Acad Sci U S A. Dec 21;96(26):14937-42.

Maldarelli F, Martin MA, Strebel K (1991). Identification of posttranscriptionally active inhibitory sequences in human immunodeficiency virus type 1 RNA: novel level of gene regulation. J Virol. Nov;65(11):5732-43.

Martoglio B, Graf R, Dobberstein B. (1997). Signal peptide fragments of preprolactin and HIV-1 p-gp160 interact with calmodulin. EMBO J. Nov 17;16(22):6636-45

Mikkelsen TR, Chapman B, Din N, Ingerslev J, Kristensen P, Poulsen K, Hjorth JP. (1992). Expression of a cytomegalovirus IE-1-factor VIII cDNA hybrid gene in transgenic mice. Trans genic Res. Jul;1(4):164-9.

Mori K, Yasutomi Y, Ohgimoto S, Nakasone T, Takamura S, Shioda T, Nagai Y. (2001). Quintuple deglycosylation mutant of simian immunodeficiency virus SIVmac239 in rhesus macaques: robust primary replication, tightly contained chronic infection, and elicitation of potent immunity against the parental wild-type strain. J Virol. May;75(9):4023-8.

Pancino G, Ellerbrok H, Sitbon M, Sonigo P. (1994). Conserved framework of envelope glycoproteins among lentiviruses. Curr Top Microbiol Immunol.;188:77-105. Review.

Pasleau F, Tocci MJ, Leung F, Kopchick JJ. (1985). Growth hormone gene expression in eukaryotic cells directed by the Rous sarcoma virus long terminal repeat or cytomegalovirus immediate-early promoter. Gene 38(1-3):227-32.

Reitter JN, Desrosiers RC (1998). Identification of replication-competent strains of simian immunodeficiency virus lacking multiple attachment sites for N-linked carbohydrates in variable regions 1 and 2 of the surface envelope protein. J Virol. Jul;72(7):5399-407.

Reitter JN, Means RE, Desrosiers RC (1998). A role for carbohydrates in immune evasion in AIDS. Nat Med. Jun;4(6):679-84.

Rizzuto CD, Wyatt R, Hernandez-Ramos N, Sun Y, Kwong PD, Hendrickson WA, Sodroski J (1998). A conserved HIV gp120 glycoprotein structure involved in chemokine receptor binding. Science. Jun 19;280(5371):1949-53.

Rizzuto C, Sodroski J. (2000). Fine definition of a conserved CCR5-binding region on the human immunodeficiency virus type 1 glycoprotein 120. AIDS Res Hum Retroviruses. May 20;16(8):741-9.

Schneider R, Campbell M, Nasioulas G, Felber BK, Pavlakis GN. (1997). Inactivation of the human immunodeficiency virus type 1 inhibitory elements allows Rev-independent expression of Gag and Gag/protease and particle formation. J Virol. Jul;71(7):4892-903.

Schwartz S, Campbell M, Nasioulas G, Harrison J, Felber BK, Pavlakis GN. (1992). Mutational inactivation of an inhibitory sequence in human immunodeficiency virus type 1 results in Rev-independent gag expression. J Virol. Dec;66(12):7176-82

Schwartz S, Felber BK, Pavlakis GN. (1992). Distinct RNA sequences in the gag region of human immunodeficiency virus type 1 decrease RNA stability and inhibit expression in the absence of Rev protein. J Virol. Jan;66(1):150-9.

Srinivas SK, Srinivas RV, Anantharamaiah GM, Compans RW, Segrest JP. (1993). Cytosolic domain of the human immunodeficiency virus envelope glycoproteins binds to calmodulin and inhibits calmodulin-regulated proteins. J Biol Chem. Oct 25;268(30):22895-9.

Stephens CR, Waelbroeck H (1999). Codon bias and mutability in HIV sequences. J Mol Evol. Apr;48(4):390-7.

Takeshita T, Takahashi H, Kozlowski S, Ahlers JD, Pendleton CD, Moore RL, Nakagawa Y, Yokomuro K, Fox BS, Margulies DH, et al. (1995). Molecular analysis of the same HIV peptide functionally binding to both a class I and a class II MHC molecule. J Immunol. Feb 15;154(4):1973-86.

Thali M, Moore JP, Furman C, Charles M, Ho DD, Robinson J, Sodroski J (1993). Characterization of conserved human immunodeficiency virus type 1 gp120 neutralization epitopes exposed upon gp120-CD4 binding. J Virol. Jul;67(7):3978-88.

Tokunaga T, Yamamoto H, Shimada S, Abe H, Fukuda T, Fujisawa Y, Furutani Y, Yano O, Kataoka T, Sudo T, et al (1984). Antitumor activity of deoxyribonucleic acid fraction from Mycobacterium bovis BCG. I. Isolation, physicochemical characterization, and antitumor activity. J Natl Cancer Inst. Apr;72(4):955-62.

Trkola A, Dragic T, Arthos J, Binley JM, Olson WC, Allaway GP, Cheng-Mayer C, Robinson J, Maddon PJ, Moore JP (1996). CD4-dependent, antibody-sensitive interactions between HIV-1 and its co-receptor CCR-5. Nature. Nov 14;384(6605):184-7.

Watts C (1997). Capture and processing of exogenous antigens for presentation on MHC molecules. Annu Rev Immunol.;15:821-50. Review.

Whalen,RG and Lowrie, DB (2000). DNA Vaccines. Methods and Protocols. Humana Press. Methods in Molecular Medicine.

Willey RL, Shibata R, Freed EO, Cho MW, Martin MA (1996)
Differential glycosylation, virion incorporation, and sensitivity to neutralizing antibodies of human immunodeficiency virus type 1 envelope produced from infected primary T-lymphocyte and macrophage cultures.
J Virol. Sep;70(9):6431-6.

Wu L, Gerard NP, Wyatt R, Choe H, Parolin C, Ruffing N, Borsetti A, Cardoso AA, Desjardin E, Newman W, Gerard C, Sodroski J (1996). CD4-induced interaction of primary HIV-1 gp120 glycoproteins with the chemokine receptor CCR-5. Nature. Nov 14;384(6605):179-83.

Wyatt R, Moore J, Accola M, Desjardin E, Robinson J, Sodroski J (1995). Involvement of the V1/V2 variable loop structure in the exposure of human immunodeficiency virus type 1 gp120 epitopes induced by receptor binding. J Virol. Sep;69(9):5723-33.

Wyatt R, Kwong PD, Desjardins E, Sweet RW, Robinson J, Hendrickson WA, Sodroski JG (1998). The antigenic structure of the HIV gp120 envelope glycoprotein. Nature. Jun 18;393(6686):705-11.

Xiang Z, Ertl HC (1995). Manipulation of the immune response to a plasmid-encoded viral antigen by coinoculation with plasmids expressing cytokines. Immunity. Feb;2(2):129-35.

Xu ZL, Mizuguchi H, Ishii-Watabe A, Uchida E, Mayumi T, Hayakawa T (2001). Optimization of transcriptional regulatory elements for constructing plasmid vectors. Gene. Jul 11;272(1-2):149-56.

Zimmermann S, Egeter O, Hausmann S, Lipford GB, Rocken M, Wagner H, Heeg K (1998). CpG oligodeoxynucleotides trigger protective and curative Th1 responses in lethal murine leishmaniasis. J Immunol. Apr 15;160(8):3627-30.